

MASTER THESIS

Solvolysis of Thermosetting Epoxy Molding Compounds

zur Erlangung des akademischen Grades einer

Diplom-Ingenieurin

im Rahmen des Studiums

Technische Chemie

eingereicht von

Angela Hecke

an der Technischen Universität Graz

am Institut für Analytische Chemie und Lebensmittelchemie

in Zusammenarbeit mit Infineon Technologies Austria AG

Betreuung:

Ernst Lankmayr, Ao.Univ.-Prof. Dipl.-Ing. Dr.techn. tit.Univ.-Prof.

Josef Maynollo, Dr.

Villach, 2012

Statutory Declaration

I herewith declare that I have authored the present master thesis independently, making use only of the specified sources / resources, and that I have explicitly marked all material which has been quoted either literally or by content from the used sources.

.....
date

.....
(signature)

Acknowledgements

My utmost gratitude goes to my advisors Ao.Univ.-Prof. Dipl.-Ing. Dr.techn. tit.Univ.-Prof. Ernst Lankmayr of the Institute of Analytical Chemistry and Food Chemistry at the Graz University of Technology and Dr. Josef Maynollo of the failure analysis department at Infineon Technologies Austria AG in Villach, for their encouragement, guidance and support from the initial to the final level of this master thesis. I am profoundly indebted to the managers of Infineon Technologies Austria AG in Villach, Dipl.-Ing. Harald Kowald, Dr. Thomas Rupp and Dipl.-Ing. Josef Moser, without whose substantial help and provision of the infrastructure this project would not have been possible.

Further I want to thank the staff at failure analysis department who aided me in a variety of concerns and, though I can't mention them all by name, I want to refer in particular to Michael Inselsbacher for solving my IT problems of any type, Antia Koffler for giving me a lot of useful information about process flows, Janine Tschabuschnig and Ferdinand Schweda for consultation regarding metallization issues, Sigrid Göller for obtaining chemicals for my experiments and Gottfried Vogl for organizing the test devices.

I am grateful to my parents for enabling me an academic education and supporting me all these years as well as to Christian, my brothers Gebhard and Gerald, the rest of my family and my friends for motivating me and giving me the energy to achieve my objectives.

Angela Hecke

Villach, January 2012

Abstract

Nowadays the majority of semiconductor devices is encapsulated with thermosetting epoxy molding compounds. To enable an optical failure analysis of the dies these plastic packages are etch-opened with strong inorganic acids. Preparation artifacts such as discolorations and corrosion of the metallic components can't be avoided. The aim of this thesis is to substitute acids by solvent systems to assure an unharmed die surface. Resting on semi-empirical approaches solvent mixtures are studied. The optimization of process parameters is performed using statistical methods.

Keywords: failure analysis, package decapsulation, semiconductor device, molding compound, solvolysis, aminolysis, transfer hydrogenolysis, Hansen Solubility Parameters, design of experiments.

Kurzfassung

Heutzutage werden Halbleiterbauelemente großteils mit duroplastischen Epoxy-pressmassen verkapselt. Um die optische Fehleranalyse der Chipkomponenten zu ermöglichen, werden diese Plastikgehäuse mit starken anorganischen Säuren aufgeätzt. Präparationsartefakte wie Verfärbungen und Korrosion der enthaltenen Metallteile können nicht vermieden werden. Zweck dieser Arbeit ist es Säuren durch Lösungsmittelsysteme zu ersetzen um artefaktfreie Oberflächen zu gewährleisten. Basierend auf semi-empirischen Ansätzen werden Lösungsmittelmischungen untersucht. Die Optimierung der Prozessparameter erfolgt mit statistischen Methoden.

Stichwörter: Fehleranalyse, Gehäuse öffnen, Halbleiterbauelement, Pressmasse, Solvolyse, Aminolyse, Transferhydrogenolyse, Hansen Löslichkeitsparameter, statistische Versuchsplanung.

Contents

1	Introduction	1
2	Epoxy Molding Compounds.....	3
2.1	Chemical Composition.....	3
2.1.1	Fillers	3
2.1.2	Resins.....	4
2.1.3	Hardeners	6
2.1.4	Additives.....	9
2.2	Decapsulation Methods.....	11
2.2.1	Manual Acid Decapsulation	11
2.2.2	Automated Acid Decapsulation.....	12
2.2.3	Plasma Decapsulation.....	13
2.2.4	Further Decapsulation Strategies	13
3	Theoretical Framework	13
3.1	Solubility Parameters	13
3.1.1	Original Definition – Hildebrand Solubility Parameter.....	14
3.1.2	Extension of the Hildebrand Solubility Parameter -	16
	Molecular Interactions.....	16
3.1.3	Extension of the Hildebrand Solubility Parameter -	21
	Hansen Solubility Parameters	21
3.2	Solvolytic Types.....	26
3.2.1	Aminolysis	27
3.2.2	Transfer Hydrogenolysis	28
3.2.3	Combination of Amines and Hydrogen Donors.....	30
3.2.4	Sub- and Supercritical Fluids	30
3.2.5	Surfactants.....	31

4	Experimental Setup	33
4.1	Devices.....	33
4.2	Sample Preparation.....	35
4.2.1	X-Ray Radiography.....	35
4.2.2	Side Cutter	35
4.2.3	Manual Grinding.....	36
4.2.4	Laser Ablation	36
4.3	Equipment.....	37
4.4	Process Flow	39
4.5	Solvent Selection.....	39
4.6	Evaluation of the Results.....	44
5	Experimental Runs and Results	45
5.1	Aminolysis.....	45
5.1.1	Diethylamine.....	45
5.1.2	Imidazole.....	47
5.2	Sub- and Supercritical Fluids.....	52
5.2.1	Water	52
5.2.2	Methanol.....	52
5.2.3	Acetone.....	53
5.3	Surfactants	55
5.3.1	Sodium Dodecyl Sulfate.....	55
5.3.2	Brij®35.....	58
5.4	Esters.....	61
5.4.1	Butyl Acetate.....	61
5.5	Phthalates.....	63
5.5.1	Diethyl Phthalate.....	64
5.5.2	Diisodecyl Phthalate	65
5.6	Multicomponent Runs	67
5.7	Design of Experiments	69
5.8	Investigation of the Die Metallization	72
6	Conclusion.....	74

Contents

Appendix	76
Acronyms.....	77
List of Symbols.....	79
Bibliography.....	81

List of Tables

Table 1: Comparison of different filler systems used for epoxy molding compound formulations. .	4
Table 2: Information about commercially available anhydride hardeners by Hitachi Chemicals. Data adapted from [5].....	9
Table 3: Hansen Solubility Parameters of cured epoxy resins. Data taken from [34] and [35].	26
Table 4: Infineon specific designation of the used devices.....	34
Table 5: Information about epoxy molding compounds of the used devices.	34
Table 6: System description of the used laser equipment.....	37
Table 7: Functional groups and molecular structures of the selected solvents and hydrogen donors.	40
Table 8: Input values for the HSPs calculations with the group contribution method for imidazole.	41
Table 9: Hansen Solubility Parameters of the selected solvents.	42
Table 10: Fractional HSPs for the selected solvents and cured epoxy resins (literature data).....	42
Table 11: Qualitative categories for the evaluation of die metallization and polyimide layer.....	44
Table 12: Input values for the HSPs calculations with the group contribution method for DIP.....	65
Table 13: Solvent mixtures for the combination runs.....	68

List of Figures

Figure 1: Schematic construction of a surface mounted device.....	1
Figure 2: Outline showing important components in the area around the die pad.....	2
Figure 3: Structures of common epoxy resins.....	5
Figure 4: Cross-linking reaction between an epoxy resin and a primary amine (hardener).....	7
Figure 5: Schematic illustration of an automatic decapsulation system [15].	11
Figure 6: Hydrogen bondings between neighboring water molecules.	20
Figure 7: Water abstraction from the secondary alcohol group of the epoxy resin [40].	28
Figure 8: Scission of the allylic bonds of the epoxy resin [40].	29
Figure 9: Proposed degradation mechanism of the phthalic anhydride hardener [40].	29
Figure 10: Front and back side of the selected test devices.	33
Figure 11: Front and back side of the test specimens after sample preparation.	37
Figure 12: Parr Pressure Vessel System as installed at Failure Analysis Department Villach. Picture taken from [55].	38
Figure 13: Left: Pressure vessel system with installed pressure gage, valve, rupture disc and thermocouple assembly. Right: Schematic cross section of the pressure vessel showing the splitting ring clasp	38
Figure 14: Ternary plot showing the fractional HSPs of the selected solvents and the cured epoxy resins.	43
Figure 15: Total Hansen Solubility Parameters of the selected solvents and cured epoxy resins... ..	44
Figure 16: Summarized evaluation of the DEA experiments.	46
Figure 17: Reflected-light micrographs of device no. 9 and 3 after treatment with a mixture of DEA and IND. The die metallization is unharmed but slightly contaminated with crystals. The polyimide layer has been removed.....	47
Figure 18: Reflected-light micrograph of device no. 9 after treatment with a mixture of IMI and NMP. The aluminum metallization has been damaged and the polyimide layer has been removed for the most part.	48
Figure 19: Left: Reflected-light micrograph of device no. 5 after aminolysis using IMI and DMF. Right: Same device after post-treatment with ethylenediamine.	49
Figure 20: Above: Reflected-light micrographs of device no. 8 after aminolysis using IMI and DETA. Below: Reflected-light micrographs of device no. 6 after aminolysis using IMI and BAL.	50

List of Figures

Figure 21: Summarized evaluation of the IMI experiments.....	51
Figure 22: Reflected-light micrographs of device no. 4 and 5 after decapsulation using a mixture of ACE and IMI. The polyimide layer was modified and remained on the die surface.	53
Figure 23: Reflected-light micrographs of device no. 7 after decapsulation using a mixture of ACE and BAL and device no. 4 after decapsulation using a mixture of ACE and DETA. The polyimide layer was preserved.	54
Figure 24: Summarized evaluation of the experimental runs using sub- and supercritical fluids...	54
Figure 25: Chemical structure of sodium dodecyl sulfate.....	55
Figure 26: Reflected-light micrographs of device no. 7 and 5 after decapsulation using SDS and BAL. The aluminum metallization is in a good condition and the polyimide layer has been preserved.	56
Figure 27: Reflected-light micrographs of device no. 8 after decapsulation using IND and SDS. All copper components reacted to copper sulfide.....	57
Figure 28: EDX spectrum of the affected die metallization of device no. 8.....	57
Figure 29: Scanning electron micrographs of device no. 8 showing the copper ball bond. Copper components are covered with copper sulfide crystals.	58
Figure 30: Chemical structure of Brij® 35.	58
Figure 31: Reflected-light micrographs of device no. 1 and 8. Left: Overview after decapsulation using BRI and BAL. Right: Overview after decapsulation using BRI and IND.	59
Figure 32: Reflected-light micrographs of device no. 1 and 4 after decapsulation using a mixture of BRI and ACE. The polyimide layer stayed unharmed.	60
Figure 33: Summarized evaluation for the experimental runs using BRI.....	60
Figure 34: Chemical structure of butyl acetate.....	61
Figure 35: Reflected-light micrographs after decapsulation using a mixture of BAT and BRI.	62
Figure 36: Reaction of BAT with ANI. Acetanilide (N-phenylacetamide) and butanol are formed.	62
Figure 37: Summarized evaluation for the experimental runs using BAT.	63
Figure 38: Chemical structure of diethyl phthalate.	64
Figure 39: Chemical structure of diisodecyl phthalate.	65
Figure 40: Ternary plot showing the fractional HSPs of the selected solvents, the cured epoxy resins and the used phthalates.	66
Figure 41: Reflected-light micrographs of device no. 1 (topchip) and device no. 8 after decapsulation using Combi 1. The polyimide layer remained on the die surface.	68
Figure 42: Predicted response graph of the solvolysis reactions using Combi 1.....	70
Figure 43: Effects Pareto chart for the number of opened devices.....	71

List of Figures

Figure 44: Effects Pareto chart for the preservation of the polyimide layer. 71

Figure 45: Effects Pareto chart for the convenience of the opening procedure. 72

Figure 46: Scanning-electron micrographs and EDX spectra of device no. 4, left after decapsulation using solvents and right after decapsulation using fuming nitric acid. 73

1 Introduction

A semiconductor device is a small electronic component, such as a transistor or integrated circuit, which is available in a discrete form. The mostly used base material is high purity monocrystalline silicon in form of a thin wafer. To protect the device against external influences it is encapsulated in thermosetting epoxy molding compounds. The electrical connection is provided by leads. A schematic construction is given in figure 1.

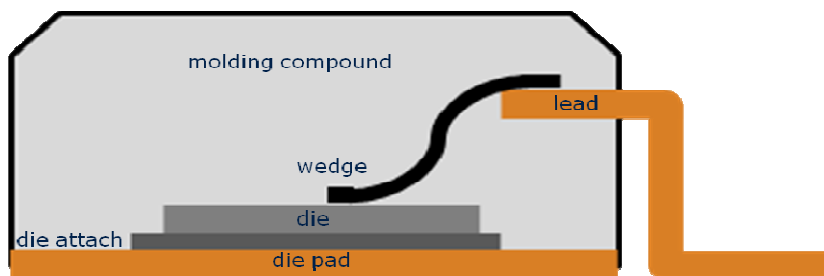


Figure 1: Schematic construction of a surface mounted device.

The fabrication of semiconductor devices is closely linked with the field of failure analysis (FA). It has become an inevitable task for the development of new products, the improvement of current ones, product qualification support but also customer returns. Different nondestructive and destructive analysis techniques, ranging from x-ray radiography, scanning acoustic microscopy and electrical measurements to focused ion beam technology and wet chemical preparation, are applied to localize and identify defects.

To enable the optical inspection or scanning-electron microscopy of the die surface and wires the epoxy molding compound in the area above the die is etch-opened with strong inorganic acids. A detailed outline of all important device components is given in figure 2. Preparation artifacts such as discolorations and corrosion of the metallic components can't be avoided.

Introduction

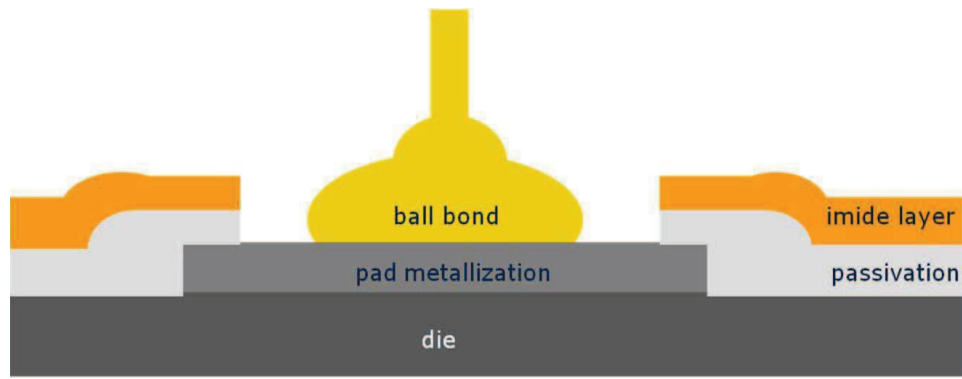


Figure 2: Outline showing important components in the area around the die pad.

The aim of this thesis is to substitute acids by solvent systems to assure unharmed die surfaces. Any preparation artifacts of the semiconductor devices should be avoided during the decapsulation process. The preparation method should consider following points:

- applicability to all chip technologies
- applicability to all types of epoxy molding compounds
- applicability to all package types
- no modification of surface structures
- little preparative effort
- reaction temperature $\leq 200^{\circ}\text{C}$
- keeping acceptable reaction times
- safe reaction system
- non-toxic agents which are easy to handle

The next chapter focuses on epoxy molding compounds and will help to gain a better understanding of the topic.

2 Epoxy Molding Compounds

2.1 Chemical Composition

By far the most common method for encapsulation of semiconductor devices is the sealing with thermosetting epoxy molding compounds (EMCs). These are composite materials which are best suited for structural applications. The main volume fraction is given by fillers, the lowest one by various additives. The core consists of a resin-hardener system, which reacts to an infusible and insoluble three-dimensional network. Nonetheless, the exact composition of an EMC formulation is a carefully guarded trade secret so that only little information about its composition is available.

2.1.1 Fillers

Filler loading plays an important part in the formulation of EMCs. It can make up to 90 wt.-%. The addition of fillers is mainly accountable for thermal conductivity of the EMCs [1], it reduces costs, increases pot life and thermal shock resistance, improves heat dissipation and dimensional stability. Further advantages are lowering of exotherms and shrinkage reduction. [2]

The type and quantity of the used filler has to be aligned to the processing conditions and the viscosity of the resin-hardener-system. It may have significant effects on thermoset morphology and adhesion properties. [2] Common filler materials are fused or crystalline silica. As semiconductor packages tend to become smaller and thinner, there is an increasing demand for high conductivity ceramic fillers such as boron nitride, aluminum oxide and aluminum nitride. In table 1 properties of various filler systems are compared. [1]

Table 1: Comparison of different filler systems used for epoxy molding compound formulations [1].

filler system	fused SiO ₂	crystalline SiO ₂	Al ₂ O ₃	SiO ₂ coated AlN	BN	Si ₃ N ₄
crystal system	amorphous	hexagonal	hexagonal	hexagonal	hexagonal	hexagonal
specific gravity [-]	2,21	2,65	3,98	3,26	1,9	3,18
thermal cond. [W/m.K]	1	10	31	195	54	26
thermal expansion [ppm/m.K]	0,5	14	7,9	4,4	40	3,5
hardness Hv [GPa]	6	10	20	12	<3	15
dielectric constant at 1 MHz	3,8	3,8-5,4	8,9	8,8	4,1	8
shape factor	spherical	regular	spherical	regular	platelet	regular
ion impurity	good	good	good	medium	bad	bad
hydrolytic stability	high	high	very high	medium	medium	very low

2.1.2 Resins

The most popular resins which are used in the semiconductor industry for molding compound formulations are epoxy resins (ERs). They consist of oligomeric or polymeric segments which incorporate more than one three-membered ring called the epoxy group. The second reactive functional group of an ER is the hydroxyl moiety. To achieve a densely cross-linked, thermosetting polymer network during the curing reaction, the quantity of functional epoxy groups has to be assured in a sufficient degree. Because ERs with miscellaneous backbone structures (see figure 3), ranging from aliphatic, cycloaliphatic to aromatic entities, are utilized for fabrication of EMCs, they can be classified according to their type of scaffold. [2] Common ERs include:

Epoxy Molding Compounds

- Biphenyl Epoxy Resin (BPE)
 - diglycidyl ether of tetramethyl biphenol
- Epoxy Novolac Resin
 - epoxy phenol novolac resin (EPN)
 - epoxy cresol novolac resin (ECN)
 - bisphenol A and F epoxy novolac resins (BPAN, BPFN)
 - multiaromatic resin (MAR)
- Hydrocarbon Epoxy Novolac Resin
 - dicyclopentadienyl resin (DCPD)
- Multifunctional Resin (MF)
 - tetraglycidyl ether of tetrakis(4-hydroxyphenyl)ethane
 - tris[4-(2,3-epoxypropoxy)phenyl]methane

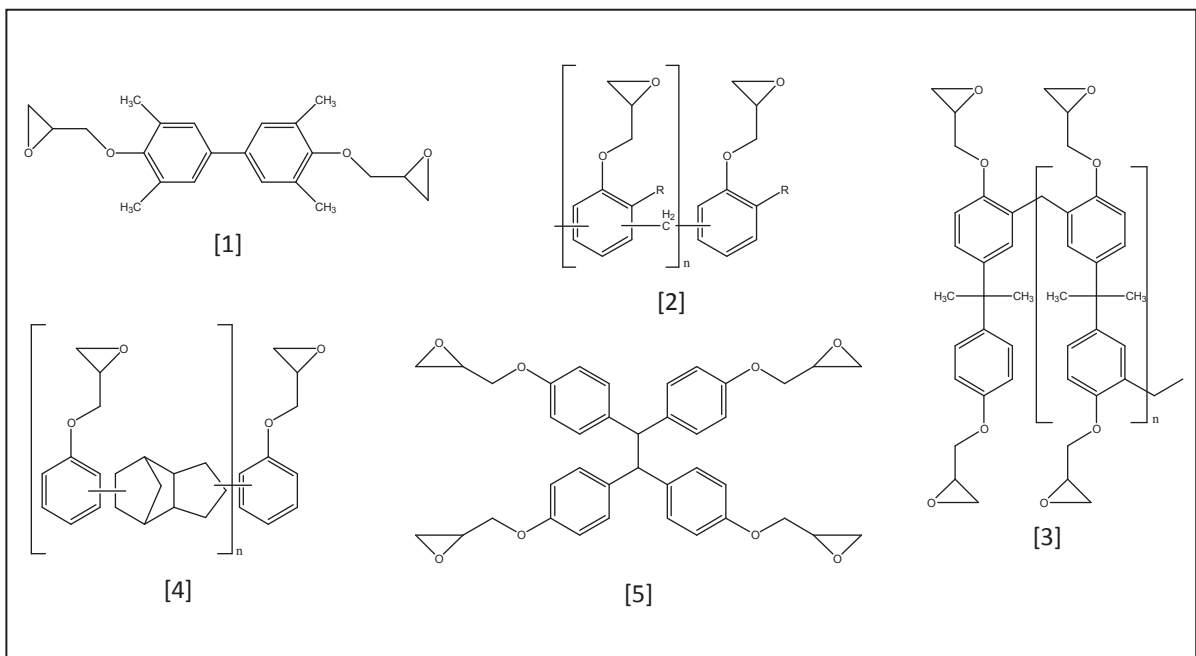


Figure 3: Structures of common epoxy resins. [1] Diglycidyl ether of tetramethyl biphenol, [2] EPN (R = H), ECN (R = CH₃), [3] BPAN, [4] DCPD, [5] tetraglycidyl ether of tetrakis(4-hydroxyphenyl) ethane.

The trend in the semiconductor industry goes to the use of crystalline epoxy resins (e.g. diglycidyl ether of tetramethyl biphenol). Due to the very low viscosity of solid, crystalline resins in their molten state a very high filler loading of up to 90 wt.-% can be achieved. This is necessary to fulfill the requirements for demanding manufacturing processes. [2]

2.1.3 Hardeners

Hardeners, also called curing agents, are cross-linkers that are necessary for converting ERs into a solid, infusible and insoluble thermosetting network. The resin-hardener-system has to be adjusted on the applied molding technique and furthermore on the resulting physical and chemical properties in order to fulfill the scope of application.

Cross-linking density is defined by the type and amount of hardener and the functional groups of the epoxy resin. Hardener and resin altogether account for 10 – 20 wt.-% of an EMC formulation. The polymerization reaction can be initiated through coreactive or catalytic pathways. Coreactive cross-linkers require active hydrogen atoms. For instance alcohols, thiols, primary and secondary amines as well as carboxylic acids and their anhydrides are applicable. They behave as a co-monomer during the polymerization reaction. (For an example of an amine-initiated curing reaction, see figure 4.) *Hitachi Chemical* for example uses alicyclic acid anhydride hardeners which have some advantages by contrast with amines. [3] For information about the characteristics of some curing agents see table 2.

In contrast, catalytic curing is performed with Lewis acids and bases. Catalytic hardeners initiate the homo-polymerization of the resin or hasten the reaction rate of additional hardeners, but they are not incorporated into the macromolecular scaffold.

Epoxy Molding Compounds

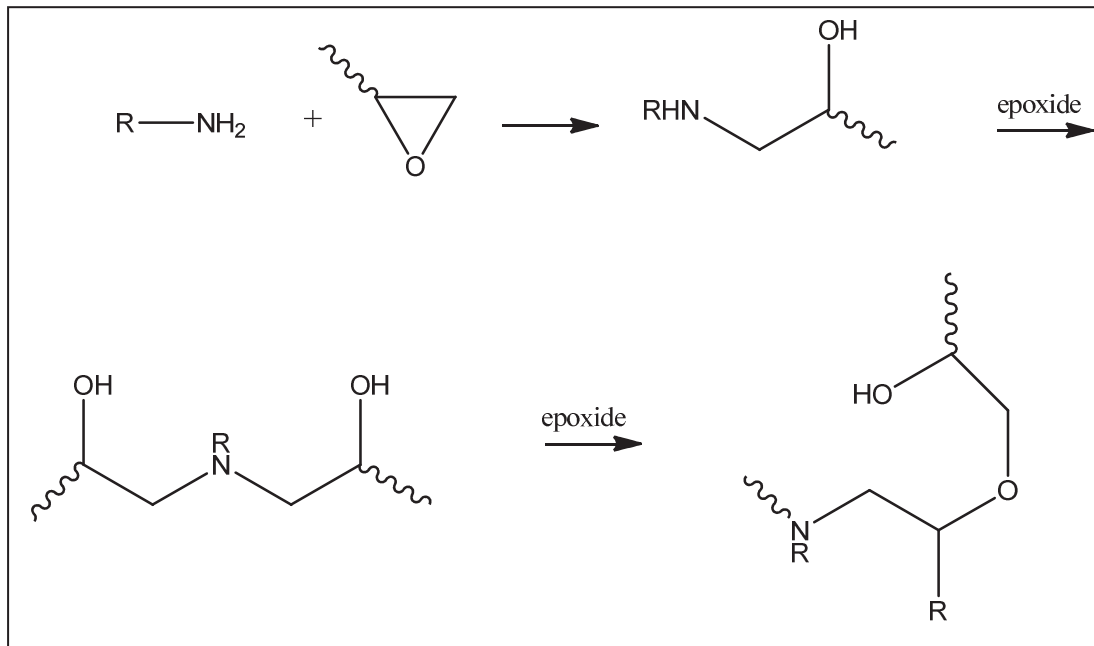
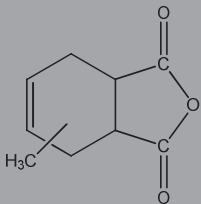
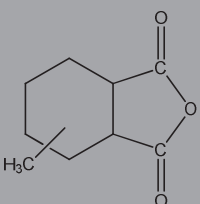
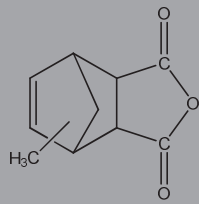


Figure 4: Cross-linking reaction between an epoxy resin and a primary amine (hardener).

The strong ring strain of the epoxy ring (see 2.1.2) enables an excellent reactivity with hardeners under several reaction conditions. The ring is opened easily, followed by the formation of linear C-O bonds. For this reason minimal shrinkage and the subsequent maintenance of the pre-molded form is ensured.

Epoxy Molding Compounds

Table 2: Information about commercially available anhydride hardeners by Hitachi Chemicals. Data adapted from [5].

Trade Name	HN-2200	HN-5500	MHAC
chemical name	3 or 4-methyl-1,2,3,6-tetrahydrophthalic anhydride	3 or 4-methyl-hexahydrophthalic anhydride	methyl-3,6-endomethylene-1,2,3,6-tetrahydrophthalic anhydride
molecular formula	$C_9H_{10}O_3$	$C_9H_{12}O_3$	$C_{10}H_{10}O_3$
structural formula			
molecular weight [g/mol]	166	168	178
appearance	colorless transparent liquid	colorless transparent liquid	light-colored transparent liquid
viscosity (mPa·s, 25 °C)	50 ~ 80	50 ~ 80	150 ~ 300

2.1.4 Additives

Additives have the task of optimizing important properties of an EMC formulation and of facilitating processability. All told, various additives amount to a maximum of 5 wt.-%. Following constituents are included: [2], [4], [5].

- Flame retardants
 - Brominated ERs, metal oxides, zinc borate, phosphorous-containing compounds.

Epoxy Molding Compounds

- Catalysts
 - Accelerate polymerization reaction, e.g. imidazoles, Lewis acids and bases (see section 2.1.3).
- Impact resistance and toughness modifiers
 - Elastomers, e.g. carboxyl terminated butadiene nitrile.
- Nonreactive diluents
 - Reduction of viscosity, e.g. nonyl phenol, furfuryl alcohol, benzyl alcohol, dibutyl phthalate.
- Stress modifier
 - Decrease Young's modulus, e.g. silicone rubber.
- Coupling agents
 - Adhesion improvement between resin and filler, e.g. silanes.
- Releasing agents
 - Advance mold release, e.g. natural or synthetic waxes.
- Pigments
 - Dyers which enhance electrical conductivity and ensure electrostatic dissipation, e.g. carbon black.

For the experimental part only “green products” were chosen. They are RoHS-compliant (for further information see directive 2002/95/EC on the Restriction of the use of certain Hazardous Substances in electrical and electronic equipment). [6] This means that they do not contain brominated ERs or any different halogenated additives, as well as any other substances of concern, especially lead or antimony containing chemical compounds [7], [8].

2.2 Decapsulation Methods

As the majority of semiconductor devices is encapsulated in plastic packages (see chapter 2.1) decapsulation techniques for metallic or ceramic sealants won't be discussed.

2.2.1 Manual Acid Decapsulation

Decapsulation of semiconductor devices is an inevitable part for the optical inspection of the dies to enable the failure localization and analysis associated with it. The standard decapsulation technique which is used at failure analysis department at Infineon Villach is the wet chemical preparation. In this regard, a distinction can be made between total and partial decapsulation strategies. If the device has just to be checked visually, the package can be removed totally by dissolving it in hot fuming nitric acid. But in the majority of the cases partial decapsulation is the method of choice. This treatment has the advantage that the interconnections are preserved and the functionality of the die is maintained. The process runs as follows:

Firstly, the EMC in the area above the die is ablated with a YAG laser (neodymium-doped yttrium aluminum garnet laser) down to a minimum height of 50 - 100 μm [9]. In some special cases the package stability can't be guaranteed by the use of laser preparation, particularly if small packages which are incorporating big dies are handled. This concern can be remedied by soldering the die pad and leads onto an acid-resistant carrier-material preliminary to the opening procedure. [10]

The second task is the manual wet-chemical etching of the remaining EMC until the entire chip surface is unveiled. Devices which are incorporating aluminum (Al) and gold (Au) metallizations and wires can be treated with fuming nitric acid at a temperature of up to 90°C because they provide a sufficient resistivity against this acid. Due to the acid's powerful oxidization properties towards the resin-hardener system the remaining EMC coating can be removed rather quickly [11]. Afterwards the polyimide layer may be removed. The device is cleaned, dried and ready for the visual analysis.

In the last years the use of copper (Cu) for construction of components of the devices, like wires, metallization or lead frames, has become more and more popular [12, 13]. Cu possesses clear advantages in comparison with conventionally applied metals (Al, Au) such as high ampacity, low resistivity, higher mechanical strength and hardness [12]. Reliability risk is reduced because the formation of intermetallic phases between Al and Cu is slower in comparison to Al and Au [14]. But Cu is severely attacked by fuming nitric acid. Therefore concentrated sulfuric acid has to be added in large quantities and process temperature has to be decreased to a maximum temperature of 45°C.

2.2.2 Automated Acid Decapsulation

As an alternative to manual etching methods automated jet etching systems, e.g. Nisene JetEtch, were developed [15]. The semiconductor package lies upside down on a gasket with an inner opening size in the dimension of the die and is fixed onto a block. This block incorporates a jet, which injects acid mixtures of nitric and sulfuric acid to dissolve the EMC. Simultaneously waste acid and debris are drained through lateral boreholes (see figure 5) [16]. Through controlled acid attack the surfaces are in a clean and better condition in comparison to manual decapped ones. The process itself can be influenced by varying acid mixture, volume and flow rate. Furthermore operating temperature and rubber gasket size have a big effect on the result.

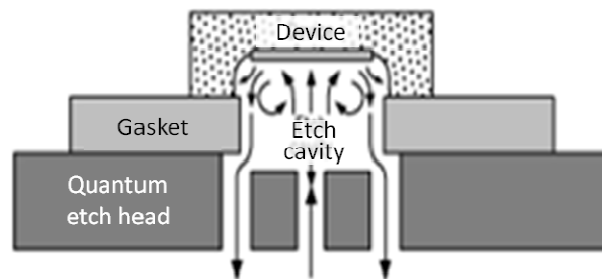


Figure 5: Schematic illustration of an automatic decapsulation system [15].

Automated etching systems are steadily refined and adjusted to the changing framework conditions. The latest automated decapping unit was developed to fulfill especially the requirements for Cu containing devices. It allows sub-room temperature acid decapsulation to avoid damage of Cu wires or metallization. For further information see SESAME 707 / 777Cu [17].

2.2.3 Plasma Decapsulation

A completely different approach for semiconductor decapsulation is the dry process adopting plasma etching, either with reactive or non-reactive ions. EMCs can be successfully etched with mixtures of oxygen (O₂) and tetrafluoromethane (CF₄). Optimization of etching recipe and process on the die technology is a very important task. Due to the use of suited gas mixtures it is possible to control material selectivity to avoid the destruction of the passivation layer and structures of the device [18, 19, 20, 21].

Plasma etching technology has a very slow etching rate, because silica fillers don't react with oxygen radicals bred in plasma. During the etching process a thin layer of silica residue is formed on the surface of the package which has to be blown away at regular intervals [19]. To minimize processing time it is advisable to previously thin the EMC in the area above the die [22].

2.2.4 Further Decapsulation Strategies

For the sake of completeness, it should be pointed out that it is also worked on various other decapsulation techniques. These include laser decapsulation [9, 23, 24, 25], mechanical and thermo-mechanical attempts [10, 26, 27, 28], the use of focused ion beam (FIB) technology [29 30], as well as numerous different solvents [10, 31, 32].

3 Theoretical Framework

Inorganic acids, which are used during standard decapsulation, can cause corrosion and discoloration of the metallic components of the dies. To avoid these artifacts so that a flawless failure evaluation is guaranteed, the idea is to substitute the applied acids with organic solvents. The aim is to select solvents which have a high affinity to the resin-hardener system of the epoxy molding compounds to dissolve it or swell it at least to a certain extent. Unveiling of the semiconductor devices should be easy to handle and universally applicable for all package types and EMC formulations. The selection is accomplished in accordance with the theoretical aspects of *Hansen Solubility Parameters* (HSPs), having regard to solvent properties like functional groups, thermal stability and vapor pressure at the test temperature.

3.1 Solubility Parameters

Solubility parameters enable an easy way for the prediction of cohesive and adhesive material properties and explain potential interactions of one substance with another. The key statement is: *“Like dissolves like.”* It is not necessary to know the precise attributes of a given system. The characteristics of a composition which has to be investigated can be prognosticated only with the knowledge of its components.

Solubility parameters were developed to determine the behavior of liquids and have now been extended to describe solids, gases and polymers.

3.1.1 Original Definition – Hildebrand Solubility Parameter

The concept of solubility is premised on thermodynamic calculations. Considering the fact that materials are more stable in condensed phase over certain temperature and pressure ranges it can be concluded that there exist energetic advantages over the gaseous state. Molecules interact with strong attractive or cohesive forces that lead to a significant negative potential energy in contrast to their gas phase. This molar potential energy is defined as the molar internal energy U , leading to the molar cohesive energy $-U$. $-U$ is defined by equation 3.1.

$$-U = {}_l\Delta_g U + {}_g\Delta_\infty U = {}_l\Delta_g U + \int_{V=gV}^{V=\infty} \left(\frac{\partial U}{\partial V}\right)_T dV \quad (3.1)$$

where ${}_l\Delta_g U$ = molar vaporization energy which is required for the vaporization of one mole of the liquid to its saturated vapor and ${}_g\Delta_\infty U$ = necessary energy for the expansion of saturated vapor until all molecules are separated at constant temperature.

At temperatures much lower than the boiling point of a liquid the second term can be neglected, leading to

$$-U = {}_l\Delta_g U = {}_l\Delta_g H - RT \quad (3.2)$$

where ${}_l\Delta_g H$ = molar vaporization enthalpy, R = universal gas constant and T = temperature.

Theoretical Framework

This stabilizing effect is expressed as the cohesive pressure, also called cohesive energy density (molar cohesive energy $-U$ per molar volume V_m), see equation 3.3.

$$c = \frac{-U}{V_m} \quad (3.3)$$

Based on this knowledge Hildebrand and Scott defined the so called Hildebrand Solubility parameter as the square root of the cohesive pressure.

$$\delta = \sqrt{c} = \left(\frac{-U}{V_m}\right)^{1/2} = \left(\Delta_g H - RT\right)^{1/2} / V_m^{1/2} \quad (3.4)$$

For this reason the Hildebrand Parameter δ , also called total cohesion parameter, is given in the dimension of (pressure)^{1/2}, most common in (MPa)^{1/2} for a standard temperature of 298 K. Equation 3.2 and 3.4 show that it is sufficient to know the molar vaporization enthalpy and the molar volume of a liquid at the temperature of interest to calculate the Hildebrand parameter. Abundant information about these values for a variety of liquids is available in databases which makes it quite easy to gain access to this topic.

3.1.2 Extension of the Hildebrand Solubility Parameter - Molecular Interactions

The Hildebrand Solubility Parameter has a few drawbacks as it was designed to describe the behavior of nonpolar nonassociating systems. Polar forces and hydrogen bonding interactions are disregarded. To understand the attributes of all solvent classes it is beneficial to have a look on electrical properties of molecules:

A pair of charges q and $-q$ forms an electric dipole moment μ in the dimension of their distance r to each other

$$\mu = q \cdot r \quad (3.5)$$

resulting in a permanent molecular dipole moment. This is an important quantity to describe molecular interactions which directs miscibility. Permanent dipoles can be formed by polar molecules. Nonpolar solvents on the other hand can form a temporary (induced) dipole moment μ_i if their electron distribution becomes deranged due to an electric field.

$$\mu_i = \alpha \cdot \varepsilon_0 \cdot E \quad (3.6)$$

where α = electric polarizability of the molecule, ε_0 = permittivity of vacuum and E = electric field strength.

Permanent and induced dipole moments trigger three types of molecular interactions:

(1) *Dipole-Dipole Interactions*, also called *Keesom* interactions, which effect the orientation of molecules. This kind of interaction works only for molecules with permanent dipoles. One dipole forces the other one to occupy an energetically preferred place, leading to the average orientation energy $-U_o$.

$$-U_o = \frac{2 \mu^i \mu^j}{(3kTr^6)} \quad (3.7)$$

where μ^i and μ^j = permanent dipole moments of two molecules, k = Boltzmann constant, T = temperature and r = distance between two molecules.

(2) *Dipole-Induced Dipole Interactions*, also called *Debye* interactions, occur through the polarization of a polar or nonpolar molecule adjacent to a polar one. The orientation of the induced moment is not depending on the direction of the inducing moment since rotation of the inducing moment is corrected by the related electric moment. This means that dipole-induced dipole interactions are temperature independent. The resulting energy is approximated with equation 3.8.

$$-iU_i = \frac{(\alpha^j \mu^i + \alpha^i \mu^j)}{r^6} \quad (3.8)$$

where α = electric polarizability for molecule i and j , μ = dipole moment for molecule i and j and r = distance between the molecules i and j .

(3) *Induced Dipole-Induced Dipole Interactions*, also called temporary dipole, dispersion or *London* forces, have the least contribution to molecular interaction forces, but they are present between all molecules, independently from polar or nonpolar characteristics. The reason for these forces is that the electrons of one molecule move permanently, resulting in a steady electrical dissymmetry. The electron cloud of adjacent molecules is disturbed and temporary dipoles of opposite polarity are generated, which prompt intermolecular attraction forces. This effect does not average to zero because one molecule chases the other, even though each molecule has its own rotation and changes its dipole direction in line with this. The dispersion energy is approximated with equation 3.9.

$$-U_d = \frac{3 \quad i \quad j \quad i \quad j}{[2(\quad i + j)r^6]} \quad (3.9)$$

where I is the ionization potential of i and j and α = electric polarizability for molecule i and j .

For an accurate description of solvent systems it is not enough to consider dipole interactions. Lewis acid-base mechanisms and hydrogen bonding association have also to be discussed.

Lewis Acid-Base Interactions origin from electron donor-acceptor interactions. A filled electron orbital with high energy in the donor molecule overlaps with an empty orbital of low energy in the acceptor molecule. Unlike covalent chemical bonding, the electron pair (EP) is donated by one molecule instead of each molecule providing one electron. The coordination of the Lewis acid to its basic counterpart can occur via three pathways:

(a) *n-bonding*: A nonbonding EP (n electrons) of a hetero atom, e.g. oxygen, nitrogen or sulfur, overlaps.

Theoretical Framework

(b) σ -bonding: EP of a σ -bond, e.g. alkyl halides or cyclopropane, overlaps.

(c) π -bonding: π -electrons of aromatic molecules or unsaturated hydrocarbons overlap.

The acceptance of the EP can proceed with three types of empty orbitals:

(a) ν -acceptance: a vacant (ν) valence orbital of a metal ion, e.g. Ag^+ , incorporates the EP.

(b) σ -acceptance: a nonbonding σ -orbital, e.g. halogens, incorporates the EP.

(c) π -acceptance: works for π -bond systems with electron withdrawing substituents.

Lewis acid-base interactions are described with the acid-base cohesion parameter ${}^{ij}A_{ab}$.

$${}^{ij}A_{ab} = 2 ({}^i\delta_a - {}^j\delta_a)({}^i\delta_b - {}^j\delta_b) \quad (3.10)$$

where δ_a = Lewis acid cohesion parameter for i and j , δ_b = Lewis base cohesion parameter for i and j .

A large negative value of ${}^{ij}A_{ab}$ indicates exothermic behavior and predicts good solubility. It can also be used to describe ion solvation. A positive value means that mixing is hindered due to athermic or endothermic processes.

Hydrogen Bonding Interactions are a special type of acid-base association. The proton donation is performed by a Brønsted acid where a hydrogen atom, which is covalently bound to an electronegative atom, forms a second bond to another atom of high electronegativity (e.g. C, N, P, O, S or halogens). The best known type is the formation of hydrogen bonds in water.

Theoretical Framework

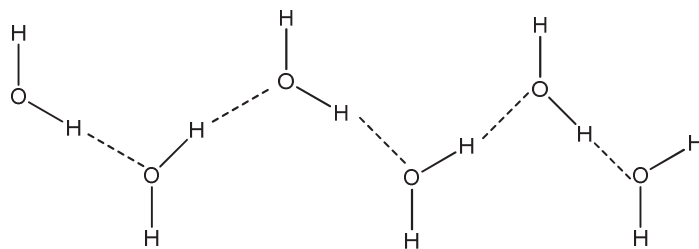


Figure 6: Hydrogen bondings between neighboring water molecules.

Pimentel and *McCellan* classified liquids into four categories, based on their role at hydrogen bonding interactions:

- (a) *Proton Donors*: provide a hydrogen atom to form the bonding, e.g. trichloromethane.
- (b) *Proton Acceptors*: molecules with electronegative atoms, which accept the hydrogen bond, e.g. aldehydes, ketones, esters, ethers or tertiary amines.
- (c) *Proton Donors/Acceptors*: incorporate the properties of both species, e.g. alcohols, carboxylic acids, water, primary or secondary amines.
- (d) *Proton Non-Donors/non-Acceptors*: liquids which are unable to form hydrogen bonds, e.g. alkanes, carbon disulfide or tetrachloromethane.

With this knowledge, it is easy to determine whether hydrogen bonding interactions contribute to the total cohesive pressure of a solvent system. Suppose that two liquids without hydrogen bonds (e.g. trichloromethane and acetone) are mixed together. In this case mixing is favored because the amount of hydrogen bonds increases during the mixing process. But if it is tried to mix a proton donor/acceptor with a proton non-donor/non-acceptor (e.g. methanol and an alkane) it can be observed that miscibility is restricted because hydrogen bonds are broken. A qualitative description of hydrogen bonding interactions may be done with the concept of Lewis acid-base interactions (see equation 3.10).

3.1.3 Extension of the Hildebrand Solubility Parameter - Hansen Solubility Parameters

Charles Hansen suggested extending the Hildebrand Solubility Parameter to a set of different interaction parameters to describe polymer-liquid interactions. He postulated that solubility of a solute in another substance, known as the solvent, is not only dependent on the total cohesive pressure of the constituents, but special value has to be set on considering the involved interaction mechanisms. Subsuming the cohesive energies of orientation (see equation 3.7) and induction forces (see equation 3.8) to the polar cohesive energy $-U_p$, he stated that the total molar cohesive energy $-U_t$ (see equation 3.2) of a material consists of three components, namely the disperse $-U_d$, the polar $-U_p$ and the hydrogen bonding energy $-U_h$, which are valid simultaneously.

$$-U_t = -U_d - U_p - U_h \quad (3.11)$$

On this basis, *Hansen* developed the total Hansen solubility parameter δ_t (see equation 3.12) which consists of three terms representing the different interaction energies. (For the mathematical background, see equations 3.3 and 3.4). The total Hansen Solubility Parameter should be identical to the Hildebrand Solubility Parameter, but numerical values may differ if they are determined by different methods. If it is not explicitly noted, δ_t and δ can be seen interchangeably in the following section.

$$\delta_t = \sqrt{\delta_d^2 + \delta_p^2 + \delta_h^2} \quad (3.12)$$

Theoretical Framework

where δ_d = Hansen Solubility Parameter for disperse interactions, δ_p = Hansen Solubility Parameter for polar interactions and δ_h = Hansen Solubility Parameter for hydrogen bonding interactions.

The central statement of this theory is: the better the conformity of δ_d , δ_p and δ_h of a polymer and the solvent, the more likely is its solubility. Hansen Solubility Parameters for a great variety of liquids are listed in [33]. If no information about these values can be found it is quite easy to calculate them using the group contribution method.

To get a spatial imagination of polymer-liquid interactions it is helpful to study the concept of the “solubility sphere”. The parameters ${}^j\delta_d$, ${}^j\delta_p$ and ${}^j\delta_h$ of the polymer j are positioned in the center of the three-dimensional space and j forms an interaction radius jR . For liquid i to act as a solvent for j , jR has to be bigger than the distance ${}^{ij}D$ of the liquid i at position ${}^i\delta_d$, ${}^i\delta_p$ and ${}^i\delta_h$ from the center ${}^j\delta_d$, ${}^j\delta_p$ and ${}^j\delta_h$.

$${}^{ij}D = \left[4({}^i\delta_d - {}^j\delta_d)^2 + ({}^i\delta_p - {}^j\delta_p)^2 + ({}^i\delta_h - {}^j\delta_h)^2 \right]^{1/2} \quad (3.13)$$

where $\delta_{d,p \text{ and } h}$ = Hansen Solubility Parameters for polymer j and liquid i .

The relationship between the distance ${}^{ij}D$ and the interaction radius jR is called the relative energy difference (see equation 3.14). A RED value < 1 predicts good solubility, RED = 1 means a limiting case, where the solubility behavior has to be identified experimentally and RED > 1 indicates poor affinity between polymer and solvent.

$$RED = \frac{{}^{ij}D}{{}^jR} \quad (3.14)$$

Theoretical Framework

Hansen Solubility Parameters can also be used to predict the properties of binary or multi-component systems. The effective parameter δ_t is volume-wise proportional to the Hansen Parameters of its constituents (see equation 3.15). With this knowledge it is possible to adjust two nonsolvents i and j in order that their mixture becomes a solvent for polymer k .

$${}_{ij}\delta_t = \frac{{}^i\phi {}^i\delta + {}^j\phi {}^j\delta}{{}^i\phi + {}^j\phi} \quad (3.15)$$

where ϕ = volume fraction of solvent i and j and δ_t = total Hansen Solubility Parameter of solvent i and j .

This mixing rule is of great assistance in terms of substituting hazardous, expensive or scarcely manageable solvents by different ones or to align the δ_d , δ_p and δ_h parameters of the solvent to those of the polymer.

The total Hansen Solubility Parameter can also be applied on surfactants. *Little* and *Singleton* found out that δ_t of a surfactant correlates clearly with its HLB (hydrophilic-lipophilic-balance) value. This relation has been approximated by equation 2.16.

$$\delta_t = \frac{243}{54-HLB} + 12.3 \quad (3.16)$$

where δ_t = Hansen Solubility Parameter of the surfactant in $\text{MPa}^{1/2}$ and HLB = hydrophilic-lipophilic-balance value of the surfactant.

Theoretical Framework

For practical applications of the Hansen Solubility Parameters the effects of physical conditions have to be considered. δ_t is not strongly dependent on temperature. The typical deviation from room temperature is $-0.03 \text{ MPa}^{1/2}\text{K}^{-1}$. In the majority of cases an adjustment of the values is not necessary. [34] The temperature influence was neglected in the experimental part because a qualitative comparison of liquid and polymer parameters was performed where all used agents as well as the test specimens were kept at the same temperature. Therefore all values would have been decreased the same and the results would not have been impaired. Pressurization of reaction systems is a way more complicated to handle. For the pressure setting of test reactor nitrogen was used, which has a critical pressure p_c of 34 bar and a critical temperature T_c of 126 K. From these values nitrogen possesses a liquid-like molar volume and has to be treated as a supercritical fluid. Gaseous nitrogen is seen as a hypothetical dissolved liquid and has a δ value of $5.3 \text{ MPa}^{1/2}$, but compression to the supercritical state enhances its solvent power and δ has to be determined with equation 3.17.

$$\delta = \left(1.25 p_c^{1/2}\right) \left(\frac{\rho_r}{\rho_{r,l}}\right) = \delta_l \left(\frac{\rho_r}{\rho_{r,l}}\right) \quad (3.17)$$

where p_c = critical pressure of the gas, ρ_r = reduced density in the supercritical state, $\rho_{r,l}$ = reduced density of the liquid (normally about 2.7) and δ_l = total Hansen Solubility Parameter.

To estimate the deviation of the Hansen Solubility Parameter from the pure solvent to the solvent with dissolved gas, its solubility in the liquid has to be identified. *Flory* and *Huggins* approximated the gas solubility with equation 3.18.

$$\begin{aligned}
 -\log {}^j\chi_s &= -\log {}^j\chi_{id} + \left(\frac{{}^j\bar{V}}{2.30RT} \right) ({}^i\delta - {}^j\delta)^2 \\
 &+ \log \left(\frac{{}^j\bar{V}}{{}^iV} \right) + 0.434 \left(1 - \left(\frac{{}^j\bar{V}}{{}^iV} \right) \right)
 \end{aligned} \tag{3.18}$$

where ${}^j\chi_{id}$ = ideal gas solubility, when it doesn't interact energetically with the solvent (log ${}^j\chi_{id} = -2.7959$ for nitrogen at 25°C), ${}^j\bar{V}$ = average partial molar volume of the gas in the solvent (nitrogen = 32.4 cm³ mol⁻¹), R = universal gas constant, T = temperature and iV = molar volume of the liquid.

Hildebrand detected a graphical correlation of ${}^j\chi_{id}$ with the Hildebrand Parameter of the solvent. The solubility of nitrogen decreases with increasing δ .

The characteristics of the polymer play also an important role in solvolysis reactions. The higher its molecular mass, the lower is the solubility. Furthermore the modification of a polymer influences the solubility behavior. Solubility parameters were developed for amorphous macromolecules. In case of crystalline materials, the crystalline regions act like cross-links, leading to an unfavorable entropy effect which lowers molecular interactions. In the case of epoxy molding compounds where highly crystalline resins are applied and a densely cross-linked network is formed (see chapter 2.1) only swelling can be observed. It is hardly surprising that only sparse information is available about thermosetting epoxy resins. Some data can be found in [34]. A total Hansen Solubility Parameter of 26.3 MPa^{1/2} has been determined by *Hansen* for Epikote 1001, a bisphenol A – epichlorohydrin epoxy resin by studying its dissolution behavior in liquids with known δ values. *Spychaj* also dealt with Hildebrand Parameters of bisphenol A – epichlorohydrin epoxy oligomers and calculated values between 19.9 and 22.8 MPa^{1/2} for a variety of commercially available products. In contrast to this method his practical determination of the same resins resulted in values between 17 and 27 MPa^{1/2}. *Matsuura* et al. postulated a δ_t value of 22.2 MPa^{1/2} for bisphenol A – polysulfone resins. Anhydride and diethylene-triamine cured epoxy resins were calculated by Hoy's method with values between 20.3

and 21.7 MPa^{1/2}. For amine-cured epoxy resins values between 20.3 and 26.7 MPa^{1/2} can be found. As no information about the solubility parameters of epoxy molding compounds is available, these values have been taken to select adequate solvents for the experimental part (see table 3).

Table 3: Hansen Solubility Parameters of cured epoxy resins. Data taken from [34] and [35].

Resins	δ_d [MPa ^{1/2}]	δ_p [MPa ^{1/2}]	δ_h [MPa ^{1/2}]	δ_t [MPa ^{1/2}]
Epikote 1001 [34]	20,4	12,0	11,5	26,3
P-1700-pSul [34]	17,9	11,0	7,0	22,2
Epon™ Epoxy Resins [34]	18,0	6,0	8,5	20,8
DGEBA-DDM [35]	17,4	10,1	9,4	22,2
DGEBA-DDM _e [35]	15,6	8,8	9,5	20,3
TGAP-ANI [35]	16,3	13,0	13,7	24,9
TGAP-DDM [35]	16,4	15,4	13,0	26,0
TGAP-DDS [35]	16,4	15,4	14,4	26,7

Epikote 1001 = bisphenol A – epichlorohydrin epoxy resin, P-1700-pSul = bisphenol A – polysulfone resin, Epon™ Epoxy Resins = average value for commercially available liquid bisphenol epoxy resins, DGEBA = diglycidyl ether of bisphenol A, DDM = diamino diphenyl methane, DDM_e = tetraethyl derivative of DDM, TGAP = triglycidyl derivative of amino phenol, ANI = aniline and DDS = diamino diphenyl sulfone.

3.2 Solvolysis Types

Thermosetting polymers are generally known for the irreversible formation of densely cross-linked networks, which become infusible and insoluble after curing. Therefore solvolysis or decomposition of such thermosets is a very challenging task. Several attempts have been made to gain a satisfying solution for this problem, mainly for recycling reasons of the resins and other constituents of composite materials, like metals and glass fiber mats. In the following sections different solvolysis strategies are described.

3.2.1 Aminolysis

Tai et al. [36] patented a method for recycling of thermosetting materials which are constituted of epoxy resins. Their aim was to plasticize the thermoset by use of amines and reuse the decomposition products for further curing reactions. Liquefaction was accomplished with amino compounds which are capable of breaking the network structure. Anhydride cured bisphenol A resins could be successfully liquefied in a few hours with ethylenediamine at 390 K. The decomposition reaction was even accelerated by the use of xylylenediamine at 423 K. According to *Tai* any aliphatic or aromatic amino compound could be used as the decomposer, e.g. benzyldimethylamine, ethylenediamine, trimethylhexamethylenediamine, xylylenediamine, pyridine or imidazole. Among all tested amines xylylenediamine was most effective. The most exciting example was the solvolysis of a semiconductor epoxy molding compound manufactured by Toshiba. The material was shredded into pieces of about 5 mm square, mixed with the same weight of xylylenediamine and kept at 673 K for one hour, resulting in a plasticized resin material. [36]

As the goal of this thesis is to recover the dies unscathed, it is not possible to adopt these drastic reaction conditions and sample preparation technique. Only swelling behavior of the test specimens can be expected for the aminolysis runs.

3.2.2 Transfer Hydrogenolysis

Transfer hydrogenolysis is a special type of solvolysis where partially hydrogenated aromatics function as hydrogen donors. They tend to rearomatize and abstract mono-molecular hydrogen. This property enables considerably milder hydrogenation conditions in contrast with gaseous hydrogen. Common applications of hydrogen donors include the liquefaction of coal [37, 38, 39] and degradation of thermosets [40, 41, 42].

According to Braun [40], hydrogen donors, such as tetralin (1,2,3,4-tetrahydronaphthalene), 9,10-dihydroanthracene and indoline, react with phthalic anhydride crosslinked epoxy resins to mainly soluble degradation products. Through an extensive study of these reaction products a possible degradation pathway could be introduced:

At temperatures in excess of 523 K water is abstracted from the secondary alcohol group of the epoxy resin (see figure 7), followed by the homolytic scission of the resulting allylic bonds (see figure 8). Allylic bonds of the phthalic anhydride hardener are cleaved too (see figure 9). Free radicals are formed which are saturated by abstracted hydrogen atoms. It is supposed that the rate determining step is the homolytic cleavage of chemical bonds and not the velocity of the hydrogen transfer to the thermoset.

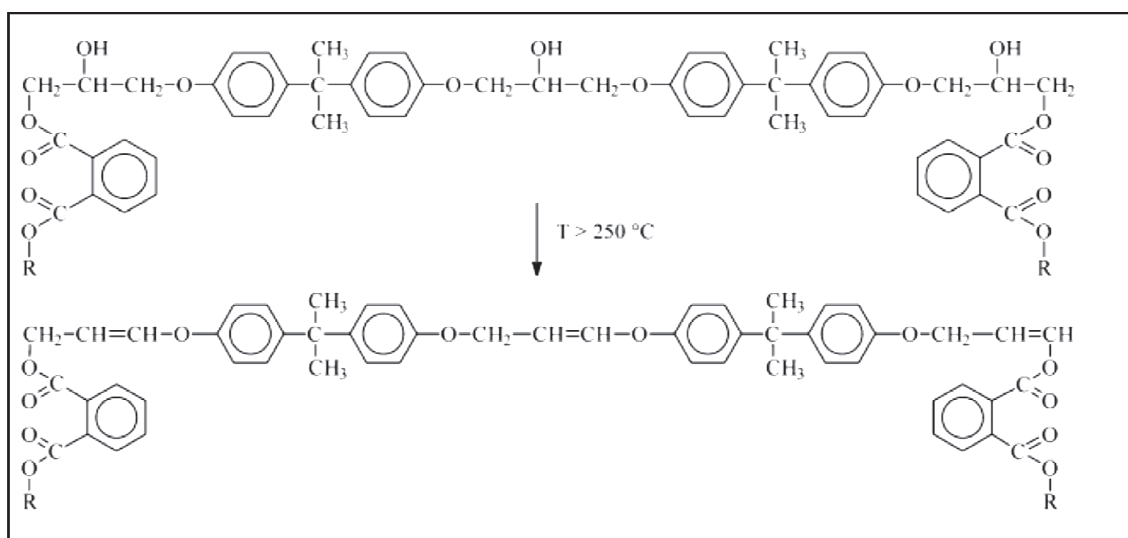


Figure 7: Water abstraction from the secondary alcohol group of the epoxy resin [40].

Theoretical Framework

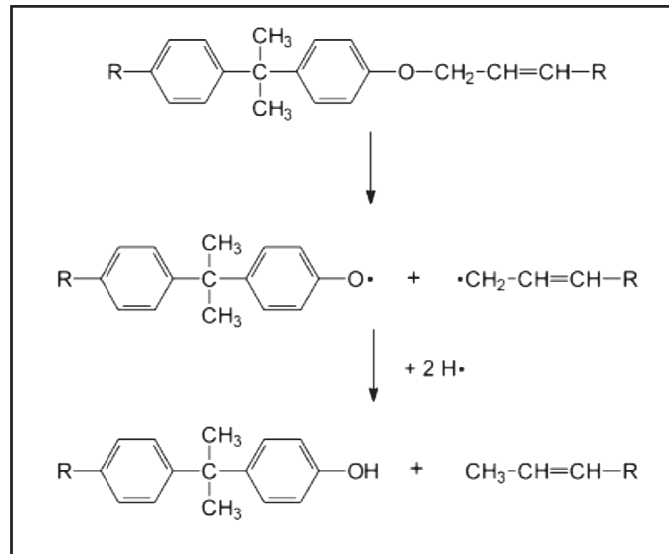


Figure 8: Scission of the allylic bonds of the epoxy resin [40].

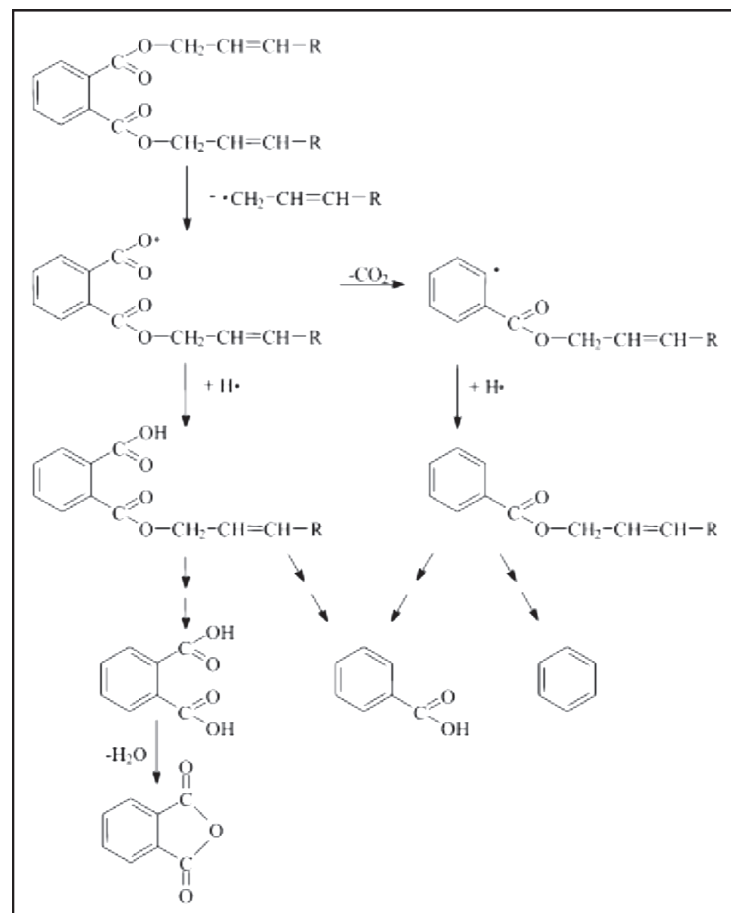


Figure 9: Proposed degradation mechanism of the phthalic anhydride hardener [40].

3.2.3 Combination of Amines and Hydrogen Donors

The reaction temperature for the hydrogenolytic degradation of thermosets can be considerably lowered through the addition of a compound with an aminic structural unit. Quantitative degradation into low-molecular weight fragments proceeds already at temperatures of 473 K. Hydrogen donors, such as tetralin, 9,10-dihydroanthracene or indoline are mixed with primary or secondary amines in a weight ratio of 5:1. The aminic compound may be any aliphatic or aromatic mono-, di- or oligoamine. Also the use of mixtures of hydrogen donors has proven most effective for solvolysis of thermosetting materials. [43]

3.2.4 Sub- and Supercritical Fluids

A supercritical fluid is any substance that is applied above a certain combination of pressure and temperature, called the critical point. From this point it cannot be differentiated between distinct liquid and gas phases. Exceptional material properties are obtained because the substance acts as a solvent and reactant. Viscosity is lowered and mass transport coefficients and diffusivity are increased, resulting in excellent solvation capabilities [44]. The term “subcritical” refers to the physical state between the boiling and the critical point.

Sub- and supercritical fluids have gained a lot of attention for the recycling of polymer wastes. Especially small molecules whose supercritical condition can be achieved with little effort, like water and alcohols, are applied.

Pinero-Hernanz et al. [44] postulated a method for the recycling of carbon fibre composites using methanol, ethanol, 1-propanol or acetone, whose critical state is easier to achieve in contrast with water [45]. Among them, acetone was best suited for solvolysis of reinforced epoxy resins because its Hildebrand Parameter of $20.0 \text{ MPa}^{1/2}$ lied closest to the parameter of the polymer. The addition of alkali catalysts, e.g. NaOH, KOH and CsOH, has proven to be advantageous. The degradation process was improved by increasing the total rate of reaction. Unfortunately, it is not possible to add catalysts for the solvolysis of semiconductor epoxy molding compounds as they would severely damage the metallic components of the devices.

Several attempts have also been made with sub- and supercritical water for the recycling of polymer wastes, including the degradation of epoxy resins [46], phenolic resin [47], condensation polymers with ether, ester or acid amide linkages [48] or printed circuit boards [49].

3.2.5 Surfactants

The bulk properties of a supercritical fluid can be manipulated by the addition of surfactants. Organized molecular assemblies are formed above the so called critical micelle concentration (CMC), which enable the solvolysis of otherwise insoluble compounds. Weakly associated molecular clusters are formed which lead to a locally higher fluid density. Either the polarity of the supercritical fluid is enhanced by the addition of solvent modifiers or solute-surfactant specific interactions are constrained which enhance solvation power by the formation of hydrogen bondings or other specific chemical interactions. [50]

Theoretical Framework

Organized molecular assemblies can also be used to catalyze aminolysis reactions. Chemical processes are accelerated by the big interfacial area between the micelles and the solvent. [51]

It is believed that surfactants have a positive influence on the solvolysis of thermosetting epoxy molding compounds. They may be capable of extracting additives of the molding compounds and improve solvolysis reactions due to the lowering of the interfacial tension between solvent and solute and the removal of dissolved polymer parts from the reaction medium.

4 Experimental Setup

4.1 Devices

A set of ten different device types was chosen for each solvolysis experiment. Care was taken to ensure that the specimens differed in various features to represent a wide spectrum of characteristics. Primarily it was focused on:

- type of epoxy molding compound
- package design
- process group
- wiring

All used devices were initial ones, meaning that they had not been exposed to any stress tests or other applications before. This is a very important factor for the accurate evaluation of the experimental results because prior treatments of the devices could have caused corrosion of metallic components or embrittlement of the semiconductor encapsulant, distorting relevant results. Figure 10 shows a micrograph of the device selection and in table 4 and 5 more information about the specimens can be gained.

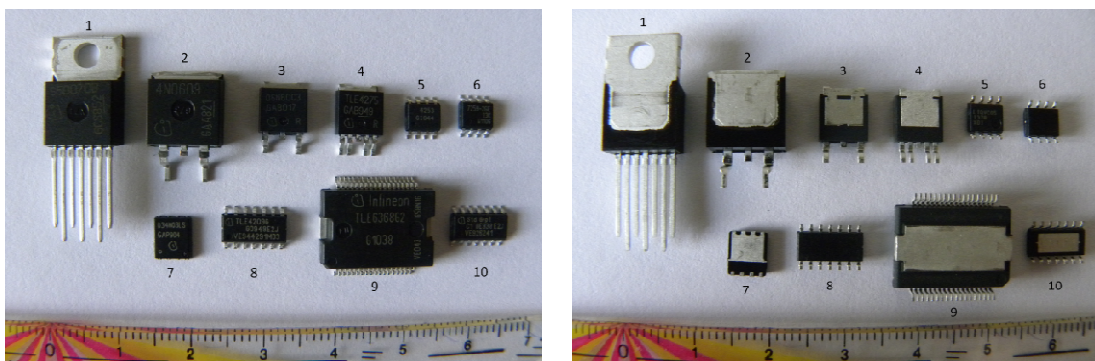


Figure 10: Front and back side of the selected test devices.

Experimental Setup

Table 4: Infineon specific designation of the used devices.

<i>Device No.</i>	<i>Sales Description</i>	<i>Package Description</i>	<i>Basic Type</i>	<i>Chip Technology</i>
1	BTS50070-1TMB	PG-TO220-7-12	U8125	SMART SIPMOS
2	IPB45N06S4-09	PG-TO263-3-2	L8954O	SFET4_8
3	SPD06N60C3	PG-TO252-3-311	L5611B	CoolMOS
4	TLE4275D	PG-TO252-5-11	S0796C	DOPL_6
5	TLE4253GS	PG-DSO-8-10	S1719A	DOPL_6
6	TLE7259-2GE	PG-DSO-8-16	S1229A	SPT_5
7	BSC034N03LSG	PG-TDSON-8-5	L8941S	SFET_4
8	TLE4209G	PG-DSO-14-22	S1787A	DOPL_4_8
9	TLE6368G2	PG-DSO-36-48	S0978W	SPT_4_8
10	BTS5020-2EKA	PG-DSO-14-40	L8300	SMART6

Table 5: Information about epoxy molding compounds of the used devices.

<i>Device No.</i>	<i>EMC Description</i>	<i>Epoxy Resin Type</i>	<i>Hardener Type</i>	<i>Supplier</i>
1	KMC 2110 G-7	modified ECN	PN	Shin Etsu
2	KMC 2110 G-7	modified ECN	PN	Shin Etsu
3	MP 8000 CH4	-	-	Nitto Denko
4	CEL 9220 HF10 KM	LMW-2	anhydride	Hitachi
5	CEL 9220 HF10 V83	LMW-2	anhydride/LWA-1	Hitachi
6	CEL 9220 HF10 V83	LMW-2	anhydride/LWA-1	Hitachi
7	CEL 1772 HF9-SS	OCN/LMW-1/Biphenyl	anhydride/LWA-1	Hitachi
8	EME G700 LX	ECN	PN	Sumitomo
9	CEL 9220 HF10 V83	LMW-2	anhydride/LWA-1	Hitachi
10	CEL 9220 HF10	LMW-2	anhydride/LWA-1	Hitachi

LMW = low molecular weight resin, OCN = ortho cresol novolac, PN = phenol novolac hardener, and LWA = low water absorption hardener.

4.2 Sample Preparation

Prior to the experimental runs all devices were modified in some degree. The extent of the preparation depended on the type of specimen.

4.2.1 X-Ray Radiography

X-ray radiography is a standard method during failure analysis of semiconductor devices. It is used for the nondestructive investigation of packages to obtain information such as position and size of dies and leads, appearance of wires, ball bonds and wedges but also to display cavities in the solder contact [52, 53]. Prior to the sample preparation all test specimens were examined radiographically to gain information about the interior of the semiconductor package. Otherwise electronic components could be severely damaged by the following preparation steps or, during manual decapsulation, by stripping off the EMC with tweezers.

4.2.2 Side Cutter

Some devices had bulky leads, which were clipped off with a side cutter (devices no. 1-4, and 9, see figure 10). Otherwise they would have occupied too much space in the reactor and therefore lowered the amount of device loading. Another advantage of this procedure was to avoid tangling up of the leads.

4.2.3 Manual Grinding

In the next step, the tin plating of exposed die pads and heat sinks was grinded off with abrasive paper (devices no. 1-4, 7, and 9-10, see figure 10). This was necessary because tin has a melting point of 505 K and reaction temperature for standard runs was 523 K. Tin would have melted and the devices would have stucked together during the cooling process. The EMC on the back side of small-sized samples (devices no. 5-6, and 8, see figure 10) was also grinded off until the lead frame emerged to facilitate handling during the opening procedure.

The front side of the test specimens was carefully roughened with the grinding paper because plastic packages are covered with waxy releasing agents which may hamper the diffusion of solvents into the polymer network.

For all grinding steps a P 180 abrasive paper of the quality SP40E by *Awuko Abrasives* was used.

4.2.4 Laser Ablation

As the diffusion of the solvent through the entire EMC is a very slow process [54], solvolysis reactions are benefited by thinner EMC layers. Packages which were covered with a thick molding compound layer (devices no. 1-4, and 9, see figure 10), were thinned with a TYREX™ - laser (Nd:YAG = neodymium-doped yttrium aluminum garnet laser) by Las Consult Leitner. For further information about the system, see table 6.

To get a better impression of how the samples look like after the preparation steps, see figure 11.

Table 6: System description of the used laser equipment.

<i>Technical Data</i>	<i>Tyrex™ - Laser</i>
laser type	diode-pumped, Q-switched Nd:YAG
wavelength	1064 nm
pulse repetition rate	5 Hz - 50 kHz
pulse duration	apprx. 10 - 20 ns
peak pulse power	80 - 250 kW
laser class	4
cooling system	entirely air cooled
pilot laser	visible, red-beam for easy positioning
software	visual laser write

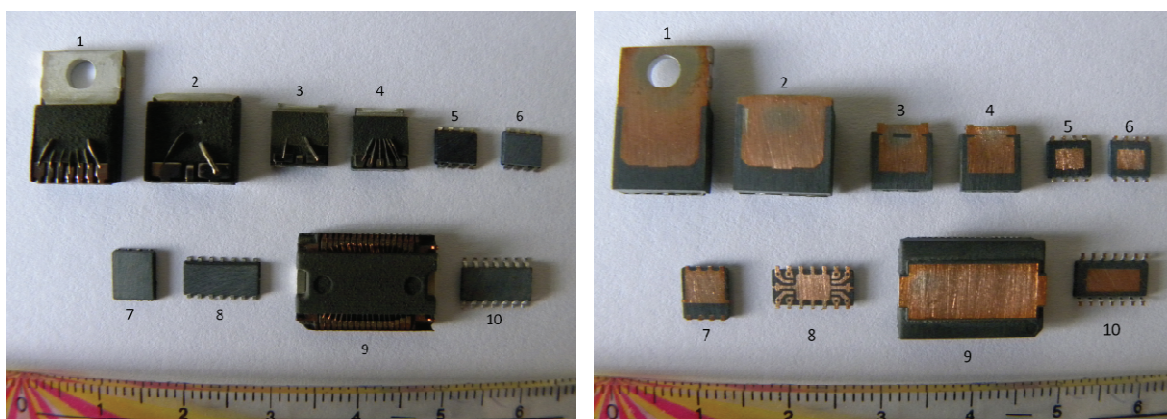


Figure 11: Front and back side of the test specimens after sample preparation.

4.3 Equipment

All experiments were conducted with a non-stirred pressure vessel system by Parr (see figures 12 and 13). This tool has been proven to be well suited for solvolysis reactions of epoxy molding compounds [55].

The main component is a 300 mL pressure reactor (model no. 4766) made of stainless steel T316 with split-ring clasp. The system is accredited to a maximum working pressure

Experimental Setup

of 200 bar and, when used with a PTFE – flask gasket, to a maximum temperature of 623 K [56]. Complete sealing of the system is provided by six cap screws. Each screw has to be tightened with a minimum of 34 Nm to compensate the tendency of the Teflon gasket to flow under pressure stress. The reactor cover is connected with a gas supply and a pressure protection system, incorporating a rupture disk. The heater (order no. A2230HCEE) is coupled with a temperature controller (order no. 4838). In addition, a glass liner was used to protect the reactor against chemical contamination.

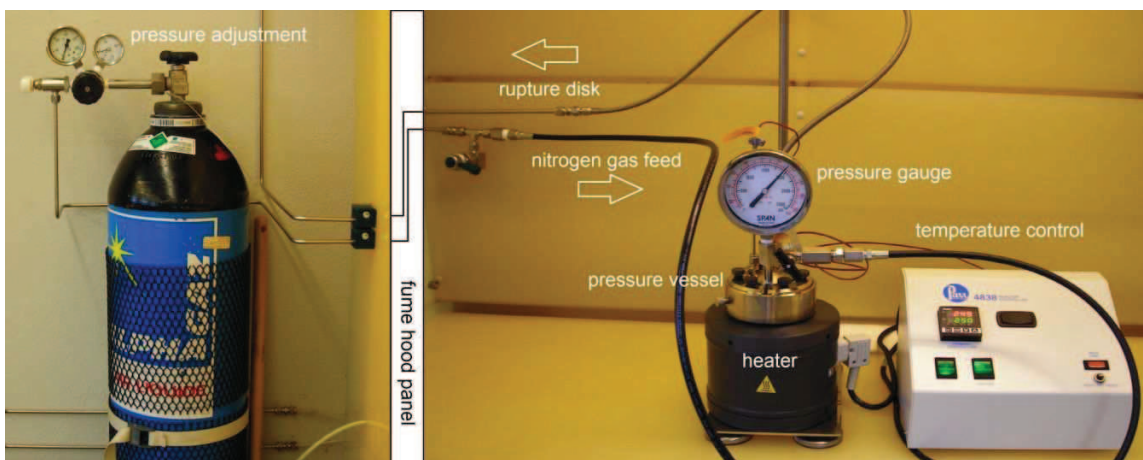


Figure 12: Parr Pressure Vessel System as installed at Failure Analysis Department Villach. Picture taken from [55].

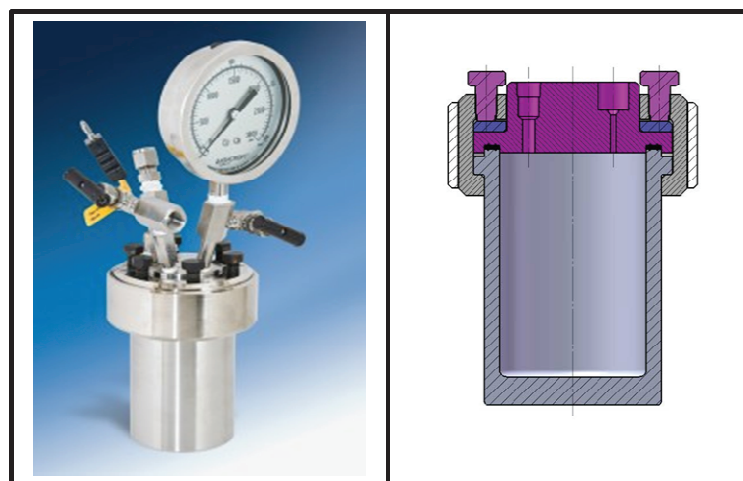


Figure 13: Left: Pressure vessel system with installed pressure gage, valve, rupture disc and thermocouple assembly. Right: Schematic cross section of the pressure vessel showing the split-ring clasp [57].

4.4 Process Flow

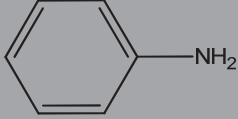
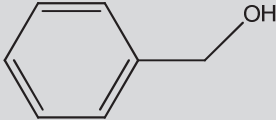
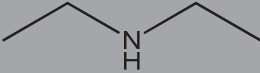
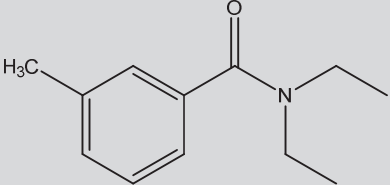
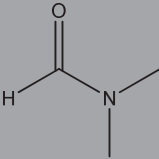
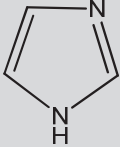
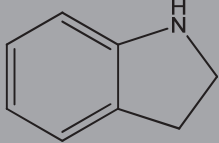
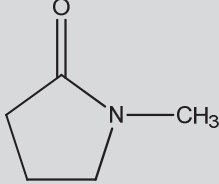
In a standard working procedure, solid reagents (imidazole, sodium dodecyl sulfate and Brij®35) are directly weighed into the glass liner of the pressure reactor. The favored quantity (50 mL for most runs) of the selected solvent mixture is added. Devices are evenly placed at the bottom of the liner, with the die pad or heat sink down. The system is assembled and screwed up, twice purged with at least 50 bar nitrogen. The desired quantity of pressure is applied and the system is heated up to the reaction temperature. Dwell time is between 7,0 and 10,0 hours. The reactor is cooled overnight, aerated and opened. Swollen EMC is removed from the die surface with tweezers. The dies are cleaned as follows: ultrasonically (US) for a few seconds in THF at room temperature (RT), US for a few seconds in warmed H_2O_{di} , blow-dried with a stream of nitrogen, US for a few seconds in THF at RT and again blow-dried. The die surface is microscopically analyzed and the quality structure of the metallization and the polyimide layer is evaluated.

4.5 Solvent Selection

A couple of different solvents and additives with a great variety of functional groups were selected for the experimental runs. A secondary aliphatic amine, namely diethylamine (DEA), and an aromatic heterocyclic one, imidazole (IMI), were chosen for the aminolysis reactions. DEA was used in pure form and in combination with different solvent types. IMI is solid at room temperature. It had to be brought into solution to avoid its precipitation into valves and cavities of the reactor cap. Therefore only combination runs were applicable. For the assortment of solvents data from prior works were taken [55]. Among them only reagents which did not attack the die metallization were chosen. These included benzyl alcohol (BAL), diethyltoluamide (DETA), dimethylformamide (DMF), N-methyl-2-pyrrolidone (NMP), aniline (ANI) and the hydrogen donor indoline (IND). The solvent functionalities and structures are listed in table 7.

Experimental Setup

Table 7: Functional groups and molecular structures of the selected solvents and hydrogen donors.

<i>Solvents & Hydrogen Donors</i>	<i>Functional group(s)</i>	<i>Molecular Structure</i>
aniline	primary amine, aromatic	
benzyl alcohol	alcohol, aromatic	
diethylamine	secondary amine	
diethyltoluamide	carboxamide, aromatic	
dimethylformamide	carboxamide	
imidazole	secondary and tertiary amine, aromatic	
indoline	secondary amine, aromatic, hydrogen donating ability	
N-methyl-2-pyrrolidone	γ -lactam	

Experimental Setup

The Hansen Solubility Parameters for the selected solvents were determined in order to compare them with the literature values of the cured epoxy resins (see table 3). Values for the total Hansen Solubility Parameter and the disperse, polar and hydrogen bonding interactions are listed in Table 9. The values for indoline and tetraline are not listed because their ability of modifying the EMC lies in donating hydrogen atoms to neutralize radicals and not in molecular interactions with the resin-hardener system (see section 3.2.2). As no literature data for imidazole was accessible, Hansen Solubility Parameter values for imidazole were calculated using the equations of the group contribution method (see equation 4.1) by Beerbower [33].

$$\delta_d = \left(\sum_z z F_d \right) / V_m \quad \delta_p = \left(\sum_z z F_p^2 \right)^{1/2} / V_m \quad \delta_h = \left(\sum_z -z U_h / V_m \right)^{1/2} \quad (4.1)$$

The used data for the calculations is given in table 8.

Table 8: Input values for the HSPs calculations with the group contribution method for imidazole.

Group	Quantity	F_d ($J^{1/2} cm^{3/2} mol^{-1}$)	F_p ($J^{1/2} cm^{3/2} mol^{-1}$)	U_h ($J mol^{-1}$)
-NH-	1	160	211	3100
>N-	1	31	149	5000
=CH-	3	223	70	0
5-membered ring	1	190	0	0

Imidazole has a molecular weight M of 68,08 g/mol and a density ρ of 1,03 g/cm³, resulting in a molar volume V_m of 66,10 cm³/mol. Using the equations (4.1) and (2.12) following Hansen Solubility Parameters are obtained:

$$\delta_d = 15,9 \text{ MPa}^{1/2}, \delta_p = 4,3 \text{ MPa}^{1/2}, \delta_h = 11,1 \text{ MPa}^{1/2}, \delta_t = 19,9 \text{ MPa}^{1/2}$$

Experimental Setup

Table 9: Hansen Solubility Parameters of the selected solvents [33, 55, 58].

Solvents	δ_d [MPa ^{1/2}]	δ_p [MPa ^{1/2}]	δ_h [MPa ^{1/2}]	δ_t [MPa ^{1/2}]
aniline	19,4	5,1	10,2	22,6
benzyl alcohol	18,4	6,3	13,7	23,8
diethylamine	14,9	2,3	6,1	16,3
diethyltoluamide	17,8	6,4	5,1	19,6
dimethylformamide	17,4	13,7	11,3	24,9
imidazole	15,9	4,3	11,1	19,9
N-methyl-2-pyrrolidone	18	12,3	7,2	22,9

The best way to compare the contributions of the molecular interactions of the solvents with those of the cured epoxy resins is a ternary plot. The HSPs are converted into fractional HSPs (see equation 4.2 and table 10) and their distribution is illustrated in a two dimensional space (see figure 14).

$$f_i = \frac{\delta_i}{\delta_d + \delta_p + \delta_h} \quad \text{for } i = d, p, h \quad (4.2)$$

Table 10: Fractional HSPs for the selected solvents and cured epoxy resins (literature data).

Solvents	f_d	f_p	f_h	cured epoxy resins	f_d	f_p	f_h
aniline	0,56	0,15	0,29	Epikote 1001	0,46	0,27	0,26
benzyl alcohol	0,48	0,16	0,36	P-1700-pSul	0,5	0,31	0,19
diethylamine	0,64	0,1	0,26	Epon™ Epoxy	0,55	0,18	0,26
diethyltoluamide	0,61	0,22	0,17	DGEBA-DDM	0,47	0,27	0,25
dimethylformamide	0,41	0,32	0,27	DGEBA-DDM _e	0,46	0,26	0,28
imidazole	0,51	0,14	0,35	TGAP-ANI	0,38	0,3	0,32
N-methyl-2-pyrrolidone	0,48	0,33	0,19	TGAP-DDM	0,37	0,34	0,29
				TGAP-DDS	0,35	0,33	0,31

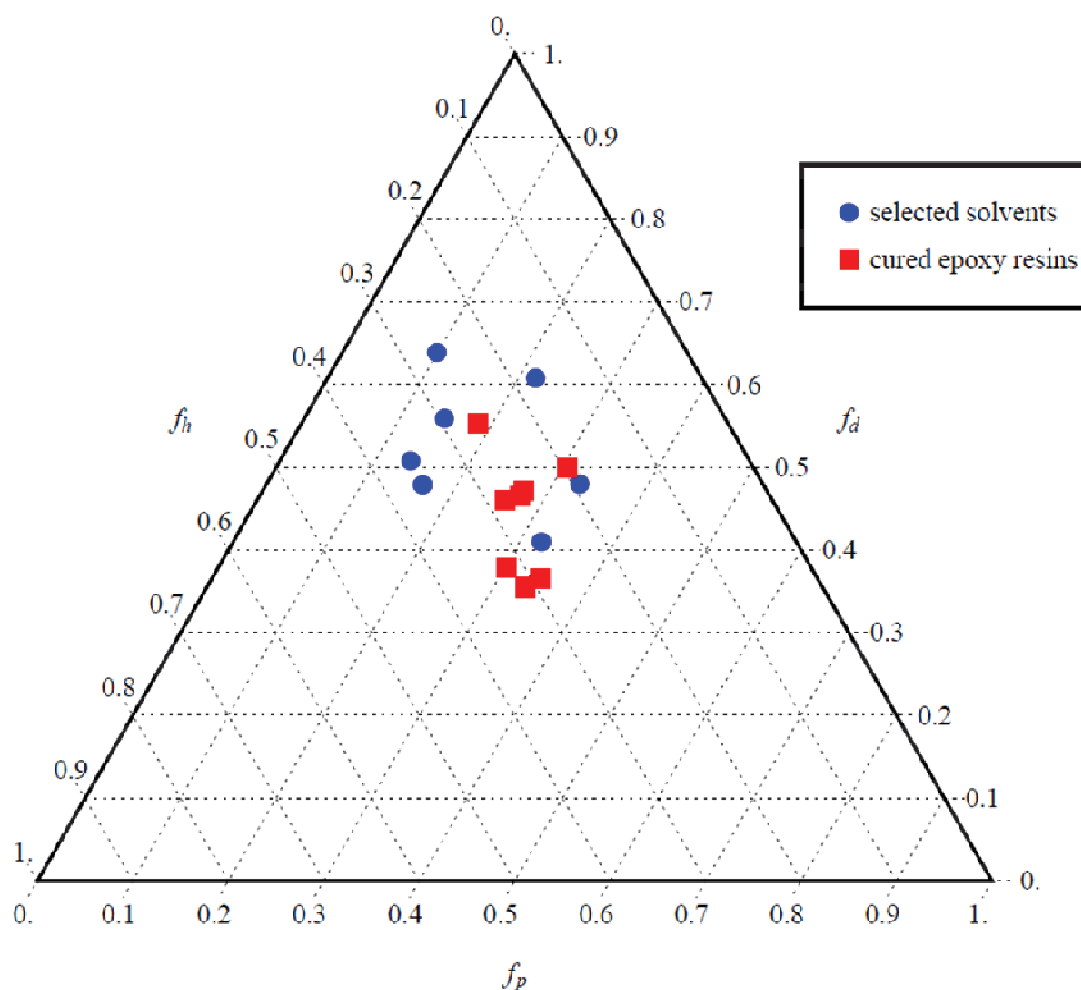


Figure 14: Ternary plot showing the fractional HSPs of the selected solvents and the cured epoxy resins.

In figure 14 it can be seen that the distribution of the fractional HSPs between solvents and thermosets is quite balanced so that solubility behavior of the EMCs can be expected. But to obtain a significant modification of the EMCs also the total HSP of the solvent has to be in the same range as that of the polymer. Cured epoxy resins have δ_t - values above $20 \text{ MPa}^{1/2}$. Among the selected solvents aniline, benzyl alcohol, dimethylformamide and N-methyl-2-pyrrolidone are most promising for the solvolysis of EMCs because they also have δ_t - values above $20 \text{ MPa}^{1/2}$ (see figure 15).

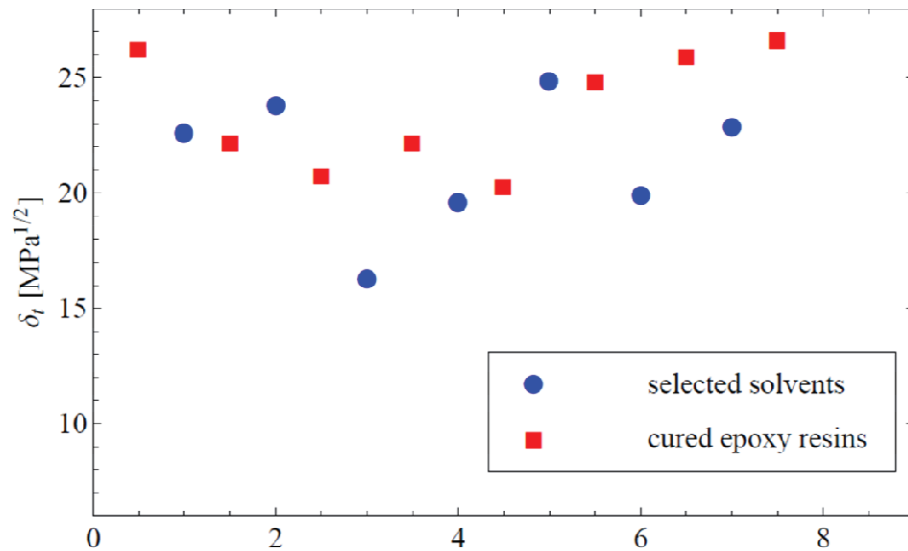


Figure 15: Total Hansen Solubility Parameters of the selected solvents and cured epoxy resins.

4.6 Evaluation of the Results

For the evaluation of the solvolysis reactions it was focused on quantitative and qualitative information that could be received from the experimental runs. One important factor was the number of decapsulated devices that indicated if the solvent mixture could be applicable for all types of EMCs and package shapes. For the qualitative evaluation the condition of the die metallization and the polyimide layer were investigated and classified into three categories, namely 3, 2 and 1 (see table 11). In case of the metallization category 3 is the best result, indicating an unharmed die surface and for the polyimide layer category 3 (complete preservation) or 1 (complete removal) are targeted. In the case of category 3, the polyimide layer can be analyzed but often category 1 is favored to facilitate the investigation of the die surface. [55]

Table 11: Qualitative categories for the evaluation of die metallization and polyimide layer.

<i>Category</i>	<i>Die Metallization</i>	<i>Polyimide Layer</i>
3	unharmed	complete preservation
2	slight discolorations	partial removal
1	severe discolorations or chemical attack	complete removal

5 Experimental Runs and Results

5.1 Aminolysis

The first experiments with the Parr Pressure Vessel were carried out with amines to check if aminolysis reactions are applicable for the decapsulation of semiconductor devices. For each aminolysis run a total solvent volume of 50 mL was used. Dwell time after reaching the wished temperature of 523 K in the interior of the vessel was 10 hours.

5.1.1 Diethylamine

Diethylamine (DEA) was tested in pure form and in mixtures of 50:50 vol%. Depending on the solvent combination the initial pressure was varied between 25 and 30 bar, resulting in about 60 – 70 bar at 523 K.

It turned out that pure DEA was not the optimal choice for dissolving semiconductor packaging materials. The devices remained hard and brittle. Adhesion between EMC, wires and polyimide layer were rather strong so that it was a challenge to unveil the dies by use of tweezers. Only six packages could be decapsulated. Die surfaces were partially contaminated with crystals, which were formed during the reaction.

The combination of DEA with aniline (ANI), benzyl alcohol (BAL) or indoline (IND) showed much better results. The EMCs became moderately soft and could be removed more easily. Nevertheless, package residues stuck on some parts of the die surface.

Package conditions after the treatment with diethyltoluamide (DETA) and dimethylformamide (DMF) mixtures could be compared with each other because the EMCs were hard but quite fragile and could be removed with light force.

Experimental Runs and Results

The best result was achieved with N-methyl-2-pyrrolidone (NMP). The EMCs were extensively swollen. No effort was needed to uncover the devices. Even some wires remained unbroken. The results for all DEA runs are summarized in figure 16.

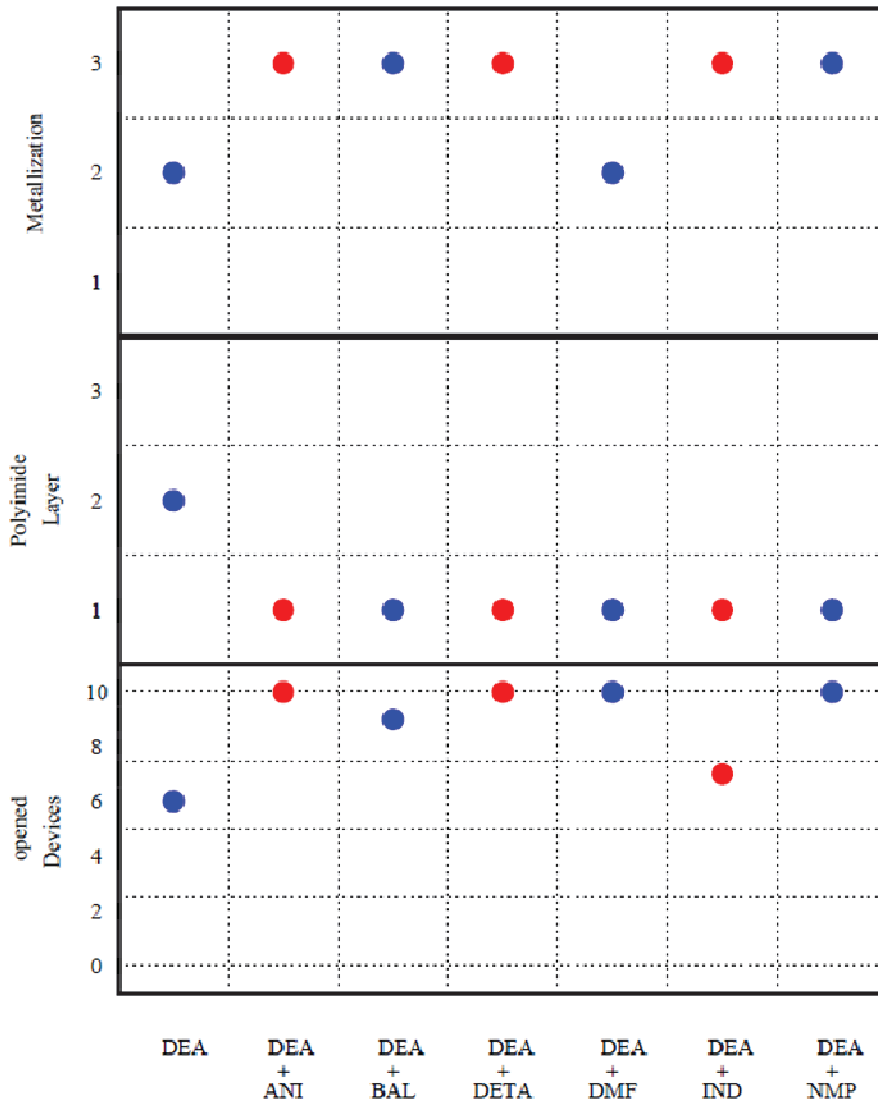


Figure 16: Summarized evaluation of the DEA experiments.

The above mentioned crystals were also more or less present at all runs performed with DEA mixtures. This amine is not suited for decapsulation of semiconductor devices

because impurities prevent an overall view of the die surface and the solvolysis effect of DEA on the EMC is quite limited because its total HSP value is too little.

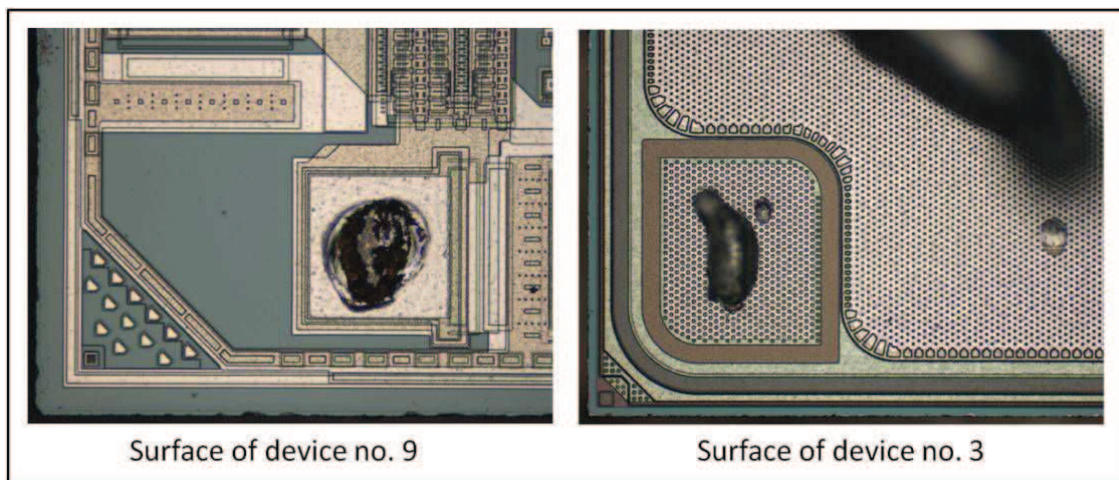


Figure 17: Reflected-light micrographs of device no. 9 and 3 after treatment with a mixture of DEA and IND. The die metallization is unharmed but slightly contaminated with crystals. The polyimide layer has been removed.

5.1.2 Imidazole

Imidazole seems to be better suited for the decapsulation of semiconductor devices because its total HSP is much higher than that of DEA.

Furthermore, IMI has been of great interest for corrosion inhibition studies of copper. From this point of view IMI is a promising candidate for copper-protecting solvolysis reactions. Its protective effect can be summarized in two steps: primarily IMI is adsorbed on the metal surface, followed by oxidation to a protective complex. This formation is favored by increasing IMI concentration and pH but impaired by raise in temperature [58].

Experimental Runs and Results

For the experimental runs 5 g IMI were dissolved in 45 mL solvent, resulting in an IMI-concentration of 1,6 mol/L. An initial pressure of 40 bar was chosen to achieve about 70 bar at 523 K. Dwell time was kept at 10 hours.

The EMCs of all devices became very soft after sample treatment with mixtures of IMI with BAL or ANI and could easily be stripped off.

IMI/DETA was a really bad combination because the packages remained very hard and were difficult to decapsulate.

DMF, IND and NMP runs had serious repercussions on device no. 9. Some parts of the pad metallization were damaged and crumbled away. An insight into the underlying layers was provided (see figure 18). Evaluation of the metallization was impossible. This phenomenon might be related to copper wire bonding. Samples, in which aluminum or gold wires were bonded on aluminum pads, stayed unharmed.

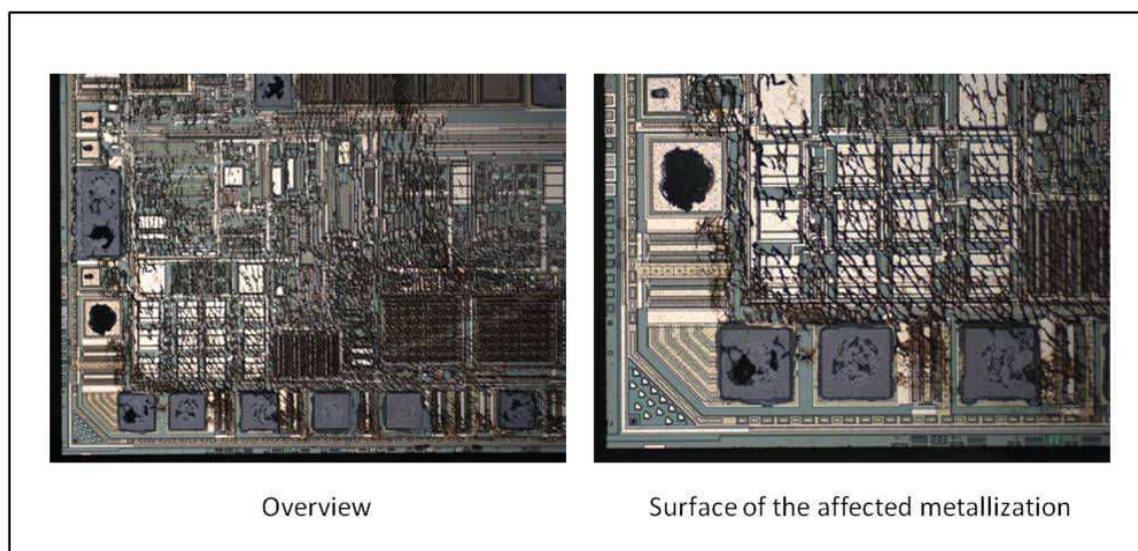


Figure 18: Reflected-light micrograph of device no. 9 after treatment with a mixture of IMI and NMP. The aluminum metallization has been damaged and the polyimide layer has been removed for the most part.

Experimental Runs and Results

Mixtures of IMI with DETA, DMF or NMP affected the polyimide layer of device no. 4 and 5 (chip technology DOPL_6). A thick black layer was formed, which could only be partially thinned after treatment with ethylenediamine for 4 h at 360 K (see figure 19). To get an idea of how severe this layer was modified during the reaction it has to be mentioned that the complete removal of polyimide layer usually needs just a few minutes.

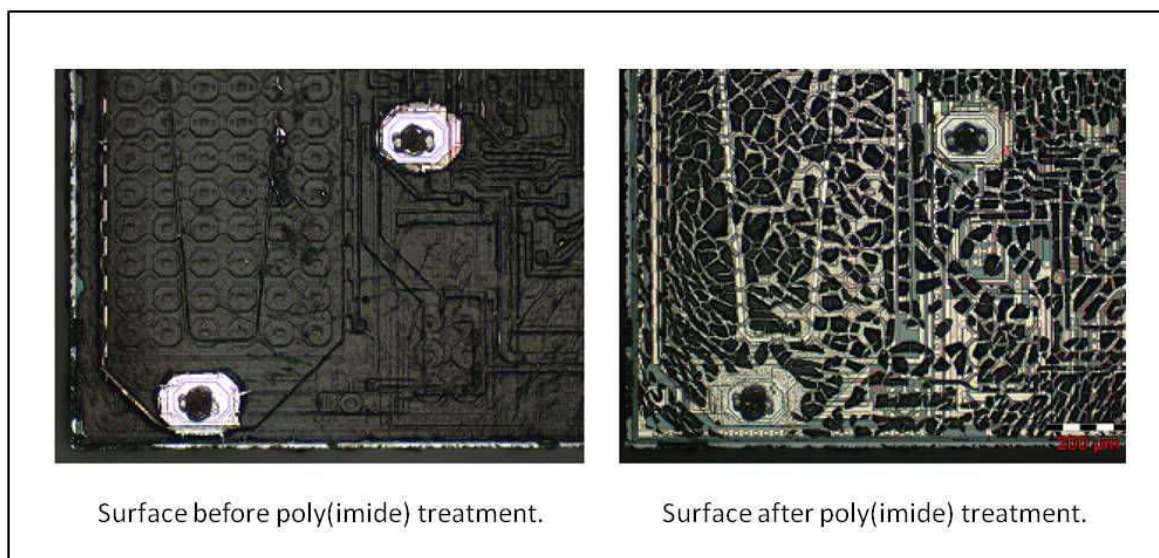


Figure 19: Left: Reflected-light micrograph of device no. 5 after aminolysis using IMI and DMF. Right: Same device after post-treatment with ethylenediamine.

The most surprising result of this series was that copper metallizations were attacked. This is the exact opposite of what has been expected. Copper surfaces were extensively discolored and oxidized. Especially the corners and edges appeared bluish due to thermal recrystallization processes of the microstructure (see figure 20, (I) and (II)).

Aluminum metallizations showed controversial results. Some of them were in a really good condition (see figure 20, (III) and (IV)). Indeed, IMI mixtures left obvious marks on some surfaces. The results for all IMI runs are summarized in figure 21.

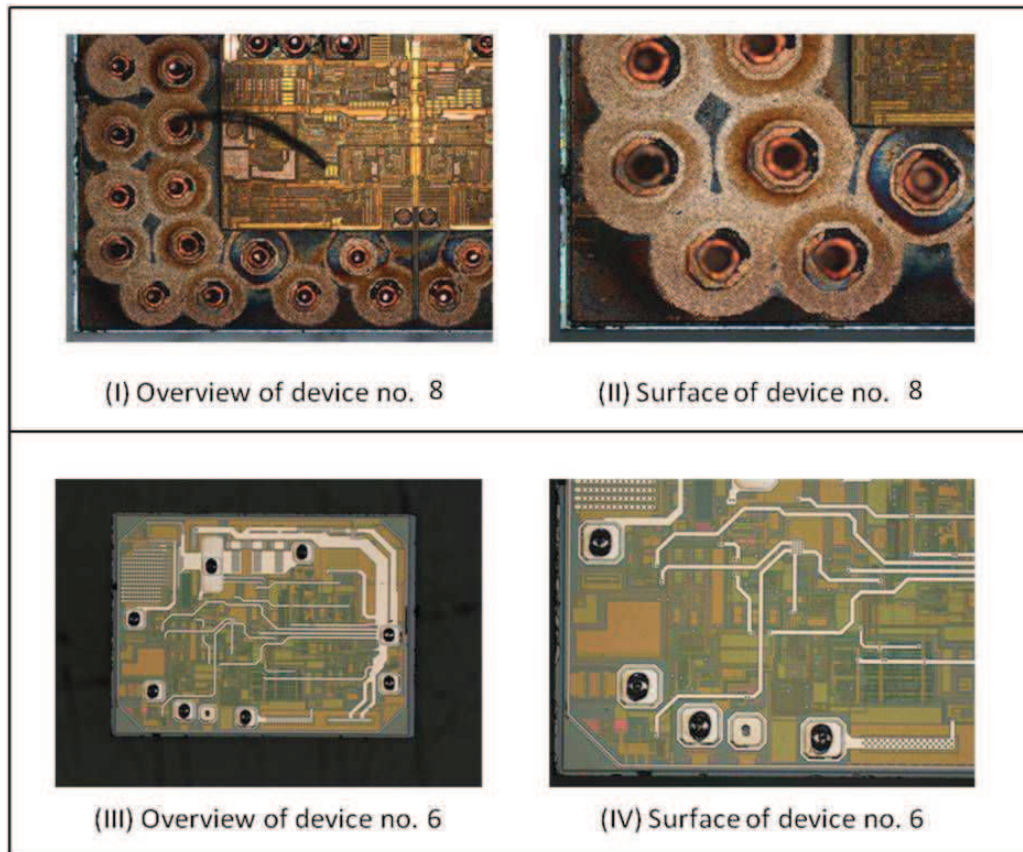


Figure 20: Above: Reflected-light micrographs of device no. 8 after aminolysis using IMI and DETA. Below: Reflected-light micrographs of device no. 6 after aminolysis using IMI and BAL.

All IMI mixtures turned dark brown due to extraction of carbon black from the EMCs. The IMI/BAL solvent system changed the most. It became a highly viscous black liquid. A possible explanation might be that further additives had been extracted.

Experimental Runs and Results

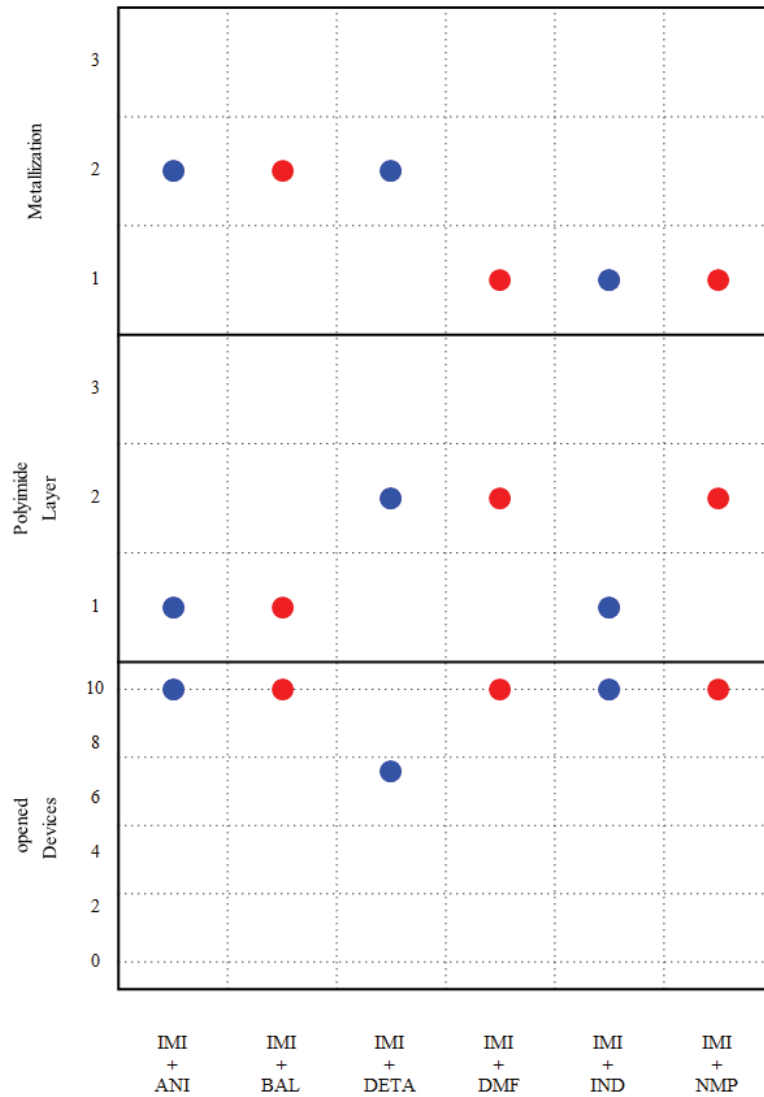


Figure 21: Summarized evaluation of the IMI experiments.

All in all it can be stated that combinations of IMI with the selected solvents can only be used in a very limited extend. Chemical attack of the metallic components can't be avoided. In most cases, all packages can be decapsulated but this fact is rather attributable to other solvents, whose total HSP values fit well together with those of the cured epoxy resins, e.g. ANI, BAL, DMF and NMP.

5.2 Sub- and Supercritical Fluids

Water, methanol and acetone were selected for the testing of sub- and supercritical solvents. Combination runs with amines and hydrogen donors were performed. The solvent volume was doubled because it is believed that it quickly becomes the limiting factor. Reaction temperature was kept at 523 K and dwell time was 10 hours. No initial pressure was applied to the reactor because sub-and supercritical fluids themselves develop a considerable pressure during heating-up.

5.2.1 Water

Water was tested in combination with IMI (5g IMI dissolved in 95 mL H₂O). This mixture was not able to swell the EMCs. They stayed extremely hard and just less than half of the packages could be decapsulated with excessive force. The die pad metallization was attacked and parts of the surface were discolored. Since water didn't show any positive effect for semiconductor decapsulation [55], no further experiments were conducted with it.

5.2.2 Methanol

The mixture of methanol with DEA in a ratio of 75:25 vol% led to embrittlement of the EMCs but didn't swell the packages. The molding compound could just be broken down piecewise. The risk of damaging the semiconductor device increased due to the necessary force for the decapsulation process. Package residues stuck on the die surfaces. The polyimide layer was partially removed. The same outcome was achieved with the

combination MeOH/IMI (5g IMI dissolved in 95 mL H₂O). The results of the methanol runs were not satisfactory.

5.2.3 Acetone

The combinations of acetone (ACE) with DEA (75:25 mL) and IMI (5g IMI dissolved in 95 mL ACE) showed better results. Although the EMCs weren't swollen they could be easier removed. In the case of ACE/IMI the polyimide layer turned black and was completely preserved (see figure 22). The die metallizations were in a better condition in comparison with water or methanol. It can be inferred that protic solvents are too aggressive for the decapsulation of semiconductor devices, but the aprotic ACE could be applied to direct the solubility behavior of the polyimide layer.

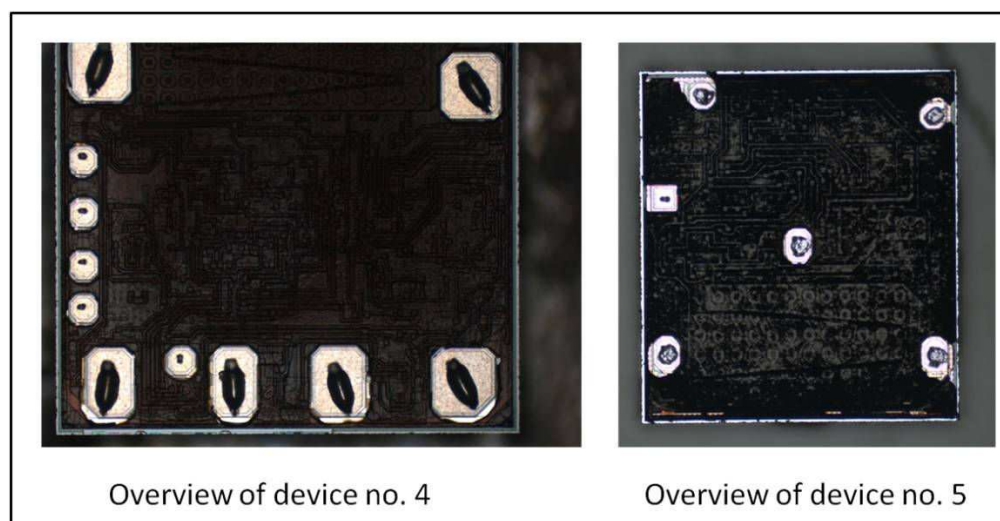


Figure 22: reflected-light micrographs of device no. 4 and 5 after decapsulation using a mixture of ACE and IMI. The polyimide layer was modified and remained on the die surface.

For this reason also combinations of ACE with ANI, BAL, DETA and NMP (75:25 mL) were tested. The presumptions that ACE can help to preserve the polyimide layer were confirmed (see figure 23). The results are summarized in figure 24.

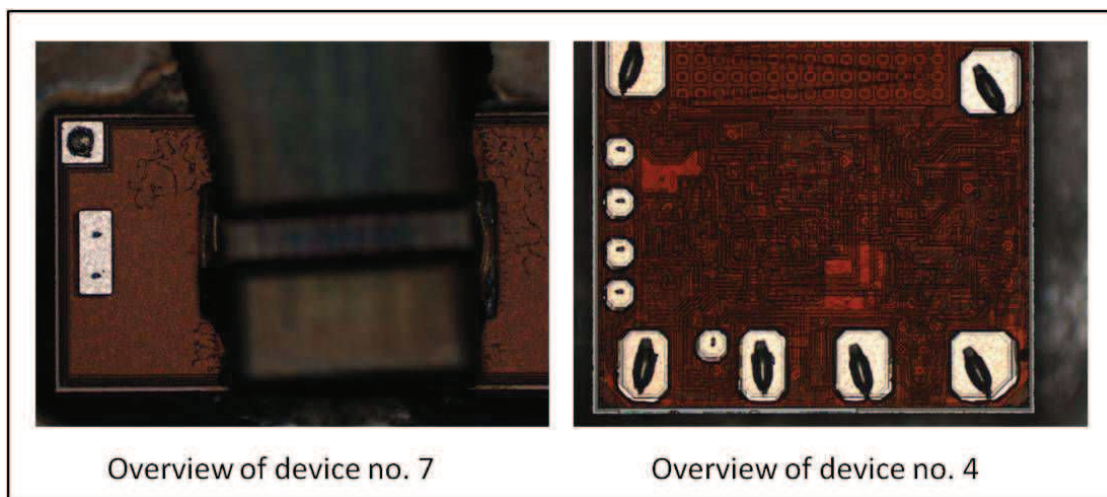


Figure 23: Reflected-light micrographs of device no. 7 after decapsulation using a mixture of ACE and BAL and device no. 4 after decapsulation using a mixture of ACE and DETA. The polyimide layer was preserved.

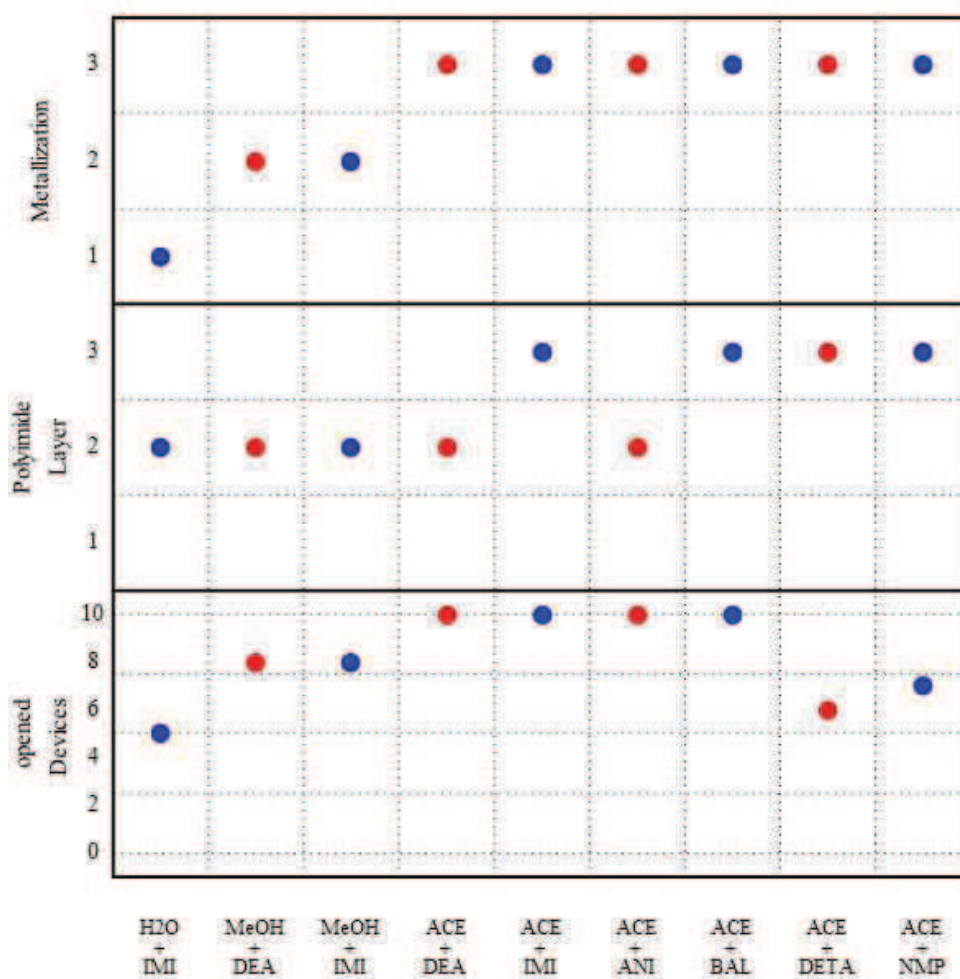


Figure 24: Summarized evaluation of the experimental runs using sub- and supercritical fluids.

5.3 Surfactants

The next experimental runs were performed with surfactants to check if their addition to the reaction media is able to enhance solvolysis reactions of EMCs (compare with section 3.2.5).

5.3.1 Sodium Dodecyl Sulfate

Sodium dodecyl sulfate (SDS) is an anionic surfactant which consists of a twelve-membered hydrophobic carbon chain attached to a hydrophilic sulfate group (see figure 25). With a HLB (hydrophilic lipophilic balance) value of 40 [59], its total HSP value of 29,7 MPa^{1/2} is calculated using equation 2.16. SDS was chosen due to its thermal stability.

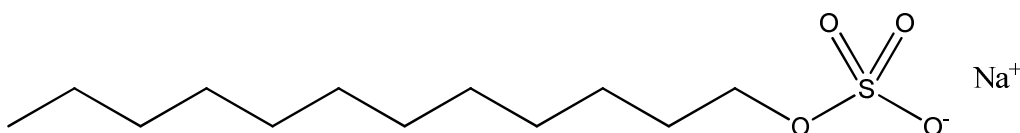


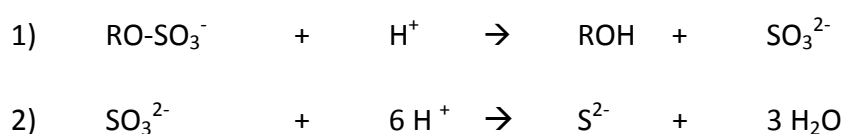
Figure 25: Chemical structure of sodium dodecyl sulfate.

For the experimental runs 1 g of SDS was dissolved in 50 mL of the selected solvent, resulting in a concentration of 69 mmol. Reaction temperature was kept at 523 K and dwell time at 10 hours. An initial pressure of 40 bar was applied to the Parr pressure vessel.

The combination of SDS with ANI, BAL, IND and NMP showed the same outcome: all packages were opened effortlessly. SDS had a very positive influence on the convenience of the decapsulation procedure. The reaction solutions turned black as SDS extracted carbon black from the EMC. The optical analysis of the devices revealed the detriment of

Experimental Runs and Results

the surfactant. Since aluminum metallizations stayed unharmed (see figure 26), copper components were all over covered with black crystals (see figure 27). For identification of these crystals an EDX analysis in the area of the copper ball bonds as well as on the power copper metallization was performed (see figures 28 and 29). Identification of the elemental composition confirmed the suspicion that copper had reacted with the sulfate group of SDS and formed copper sulfide. In accordance with [60] the occurring reaction can be described as follows:



The effect was most apparent at the combination of SDS with IND, indicating that this was the solvent mixture with the most reducing activity.

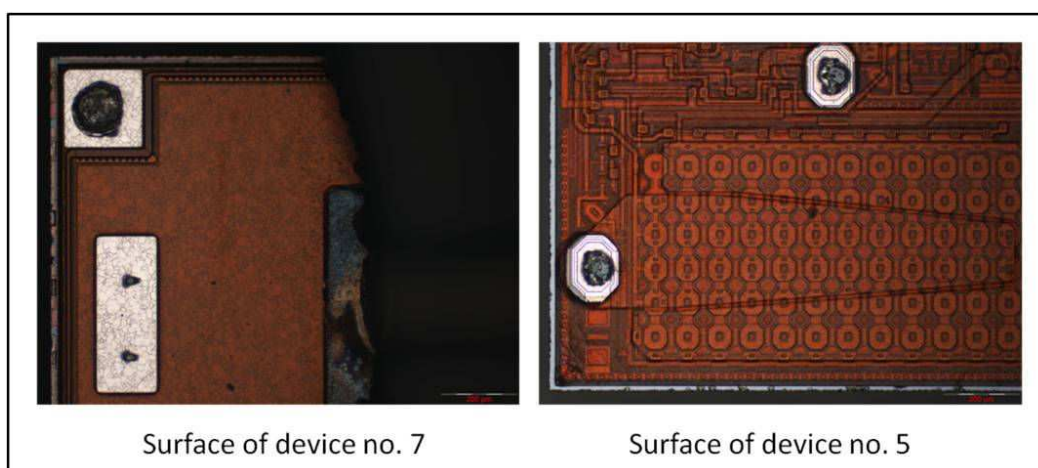


Figure 26: Reflected-light micrographs of device no. 7 and 5 after decapsulation using SDS and BAL. The aluminum metallization is in a good condition and the polyimide layer has been preserved.

Experimental Runs and Results

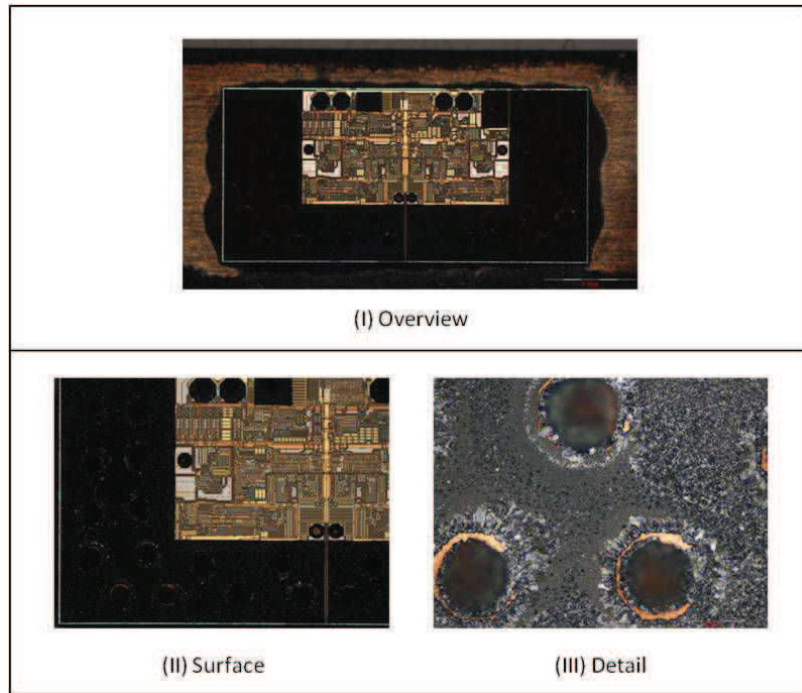


Figure 27: Reflected-light micrographs of device no. 8 after decapsulation using IND and SDS. All copper components reacted to copper sulfide.

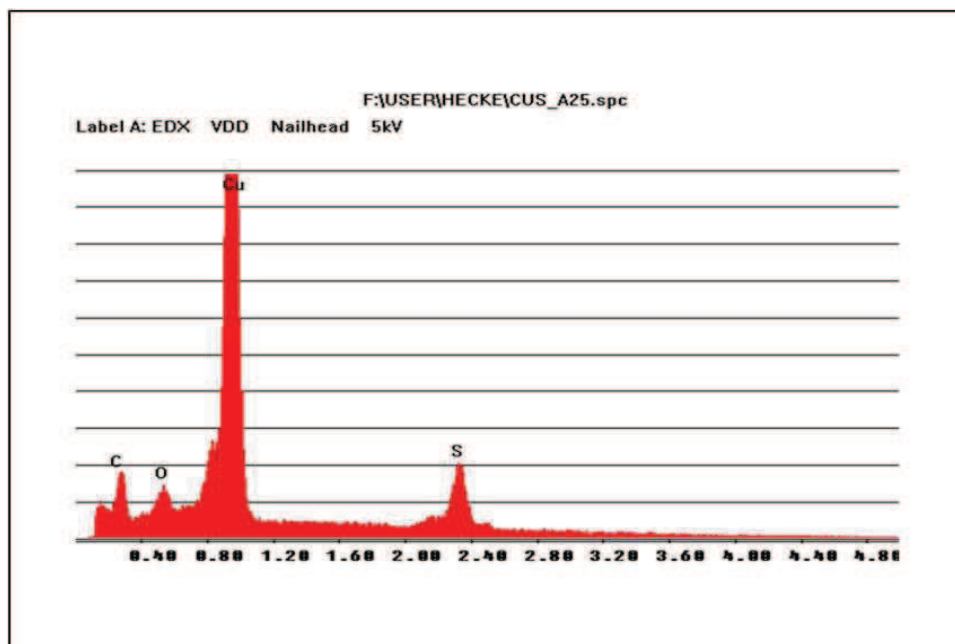


Figure 28: EDX spectrum of the affected die metallization of device no. 8.

Experimental Runs and Results

For the experimental runs 5 g of BRI were dissolved in 50 mL of the selected solvent mixture (50:50 vol%), resulting in a concentration of 83 mmol. Reaction temperature was kept at 523 K and dwell time at 10 hours. An initial pressure of 40 bar was applied to the Parr pressure vessel.

Although the EMCs became a shade less soft by use of BRI in comparison with SDS, the die metallizations stayed unharmed and the surfaces appeared very clean (see figure 31). The best results were achieved by use of BRI mixtures with ANI, BAL and IND. The EMCs were extensively swollen and quite easy to remove. It turned out that DETA had only little solvation power. For the decapsulation of all packages a cosolvent would be needed. By use of DMF all packages could be decapsulated but residues of the molding compound stucked on the die surfaces. BRI/ACE showed that the condition of the polyimide layer wasn't affected by the addition of surfactant (see figure 32). But the decapsulation of big devices was quite difficult. The results for the BRI runs are summarized in figure 33.

BRI was added to all further experimental runs as it didn't harm the die metallizations and showed a pleasant cleaning effect.

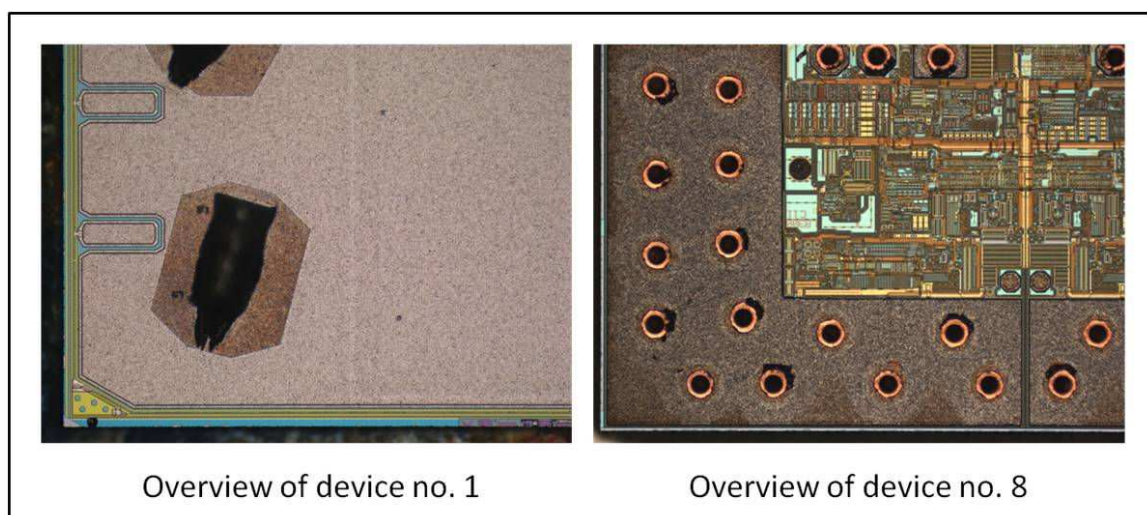


Figure 31: Reflected-light micrographs of device no. 1 and 8. Left: Overview after decapsulation using BRI and BAL. Right: Overview after decapsulation using BRI and IND.

Experimental Runs and Results

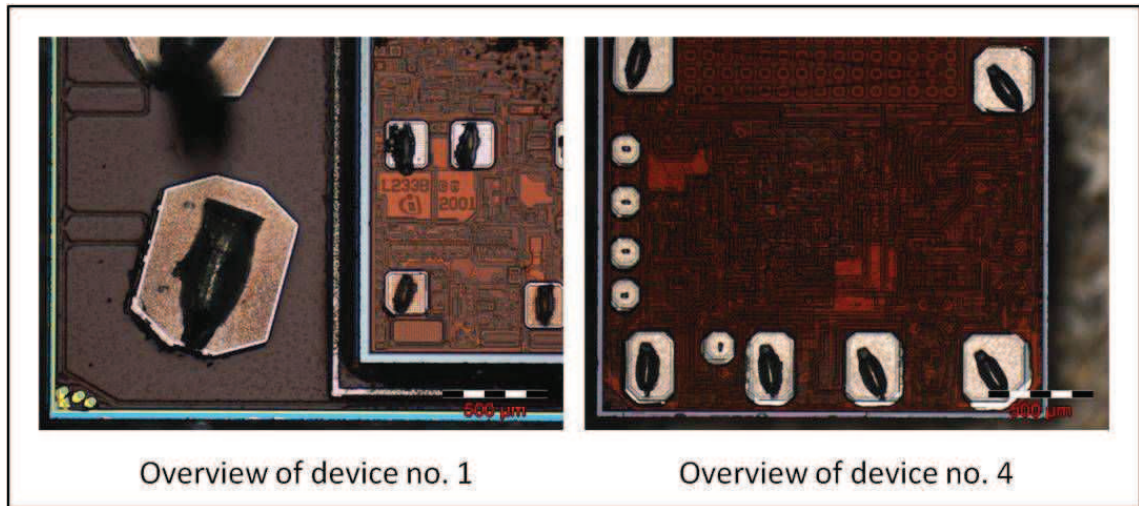


Figure 32: Reflected-light micrographs of device no. 1 and 4 after decapsulation using a mixture of BRI and ACE. The polyimide layer stayed unharmed.

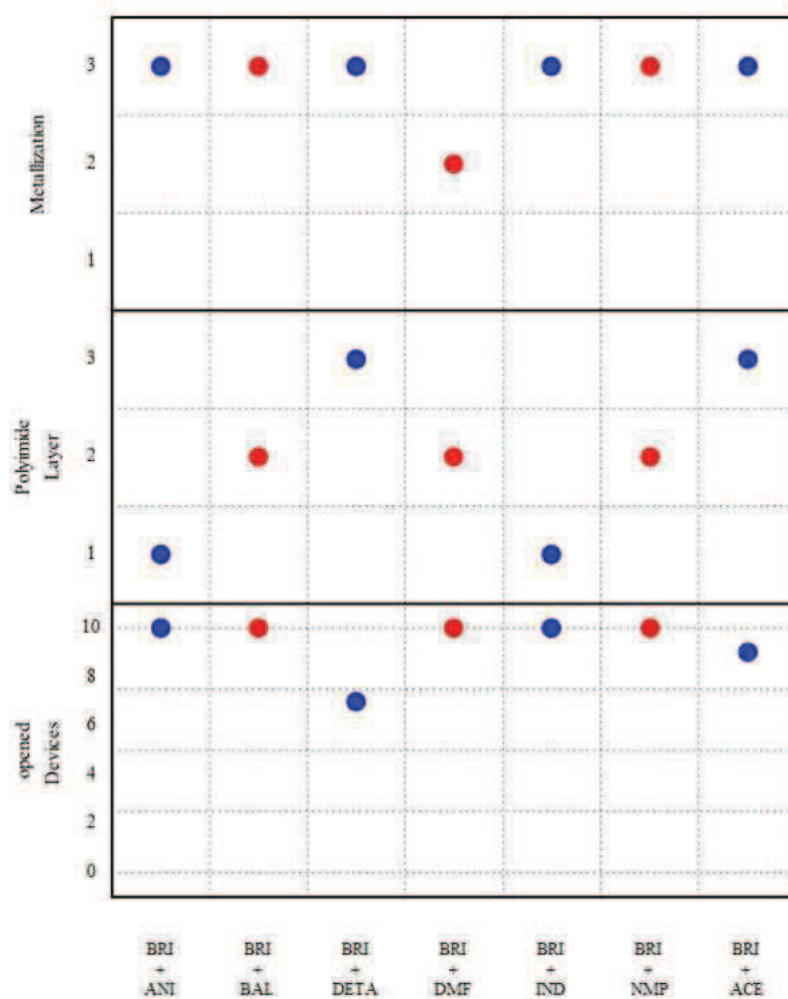


Figure 33: Summarized evaluation for the experimental runs using BRI.

5.4 Esters

Until now no information about solvolysis reactions of cured epoxy resins using esters has been reported. For this reason it was of great interest to check if esters may be applied in this field and could extend the range of chemical agents.

5.4.1 Butyl Acetate

For the investigation of the solvolysis behavior of esters butyl acetate (BAT) was selected (see figure 34). BAT has following HSPs [33]:

$$\delta_d = 15,8 \text{ MPa}^{1/2}, \delta_p = 3,7 \text{ MPa}^{1/2}, \delta_h = 6,3 \text{ MPa}^{1/2}, \text{ and } \delta_t = 17,4 \text{ MPa}^{1/2}$$

The total HSP of BAT is much lower than those of the cured epoxy resins (compare with table 3). No swelling effect can be expected. It has to be ascertained if BAT has any positive effect on solvolysis reactions.

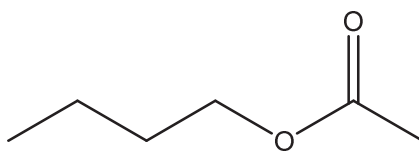


Figure 34: Chemical structure of butyl acetate.

BAT was used in pure form and in combination with different solvents in a ratio of 50:50 vol%. 5 g of BRI were added to each reaction mixture. The reaction conditions from section 5.3 were retained.

Experimental Runs and Results

The experimental runs showed that BAT didn't attack the die metallizations. The polyimide layer was preserved (see figure 35). Unfortunately only a few devices could be decapsulated because the EMC remained very hard. Thanks to the addition of solvents the number of opened devices could be increased but the convenience of the decapsulation procedure was diminished.

The combinations of BAT with ANI and IND revealed that a solvent mixture containing an ester and an amine is not applicable at the required reaction conditions because an amide which precipitates during cooling down and encases the samples and an alcohol which attacks the die metallization are formed (see figure 36). The results for all BAT runs are summarized in figure 37.

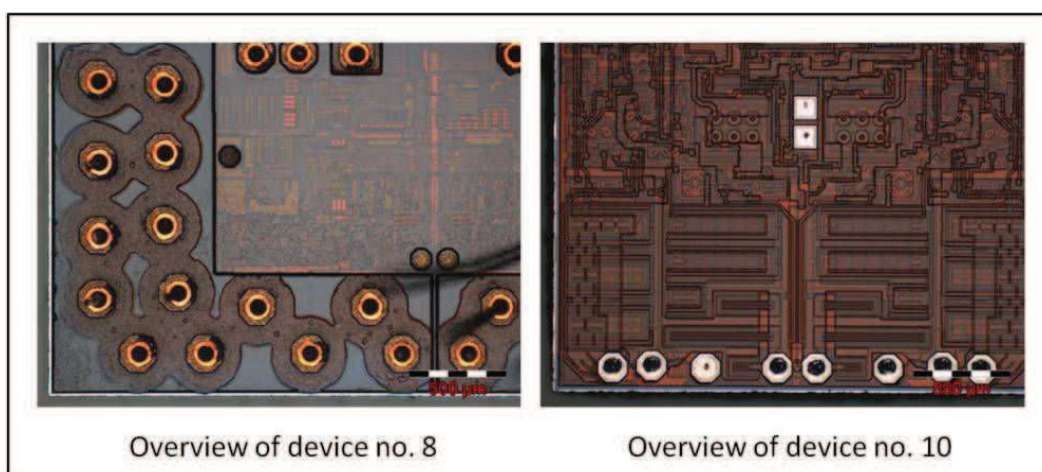


Figure 35: Reflected-light micrographs after decapsulation using a mixture of BAT and BRI.

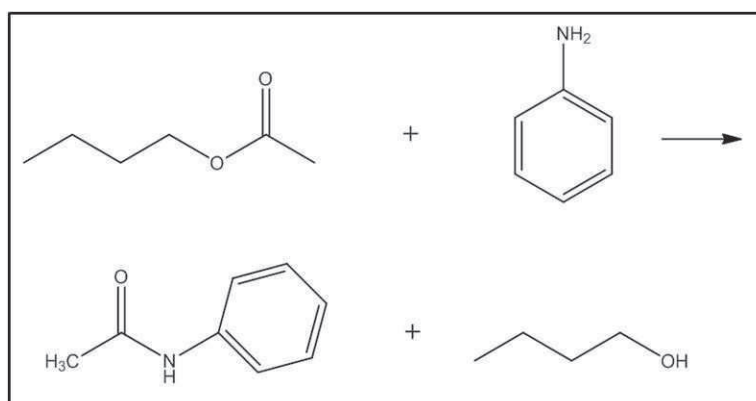


Figure 36: Reaction of BAT with ANI. Acetanilide (N-phenylacetamide) and butanol are formed.

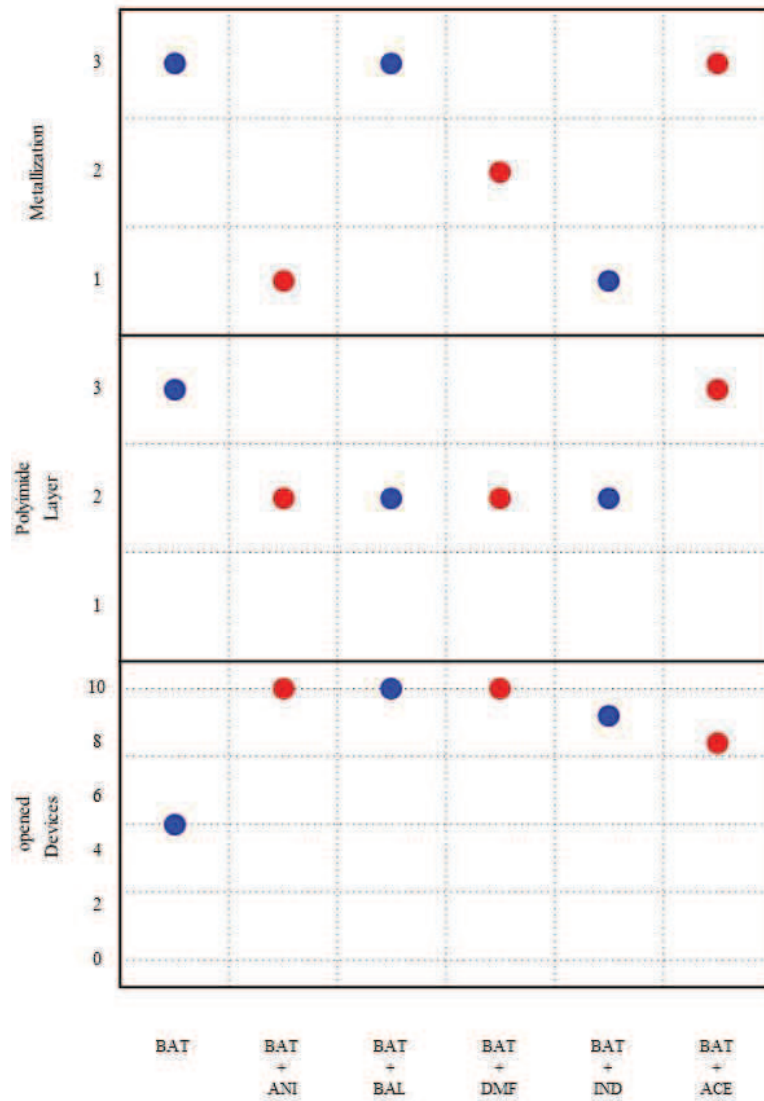


Figure 37: Summarized evaluation for the experimental runs using BAT.

5.5 Phthalates

Phthalates are commonly used as plasticizers for polymer formulations. Following advantages are obtained: processability is facilitated and the field of application is broadened. Material flexibility is increased and viscosity is lowered. The effect of phthalates on the solubility of cured epoxy resins was investigated.

5.5.1 Diethyl Phthalate

The first plasticizer which was used for the experimental runs was diethyl phthalate (DEP, see figure 38). DEP has following HSPs [33]:

$$\delta_d = 17,6 \text{ MPa}^{1/2}, \delta_p = 9,6 \text{ MPa}^{1/2}, \delta_h = 4,5 \text{ MPa}^{1/2}, \text{ and } \delta_t = 20,6 \text{ MPa}^{1/2}$$

The total HSP of DEP is of nearly similar size as those of the cured epoxy resins but its δ_h value is much smaller so that molecular interactions of DEP with the EMCs are presumably of limited nature.

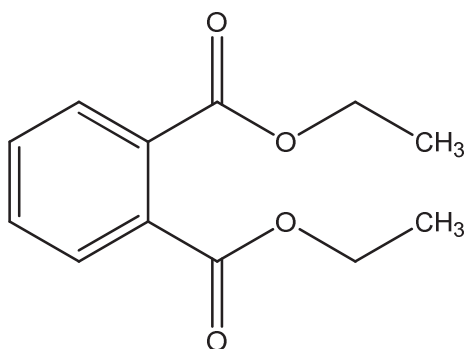


Figure 38: Chemical structure of diethyl phthalate.

DEP was tried out purely and in combination with BAL and NMP. 5 g of BRI were added to the mixtures. The reaction conditions of prior runs were retained. ANI and IND were not used because of the risk that the solvents could react with the phthalate to form amides (compare with figure 36).

5.5.2 Diisodecyl Phthalate

To increase the number of experiments with phthalates further experiments with diisodecyl phthalate (DIP, see figure 39) were performed. As no literature data for DIP was accessible, HSP values for DIP were calculated using the equations of the group contribution method (see equation 4.1) by Beerbower [33].

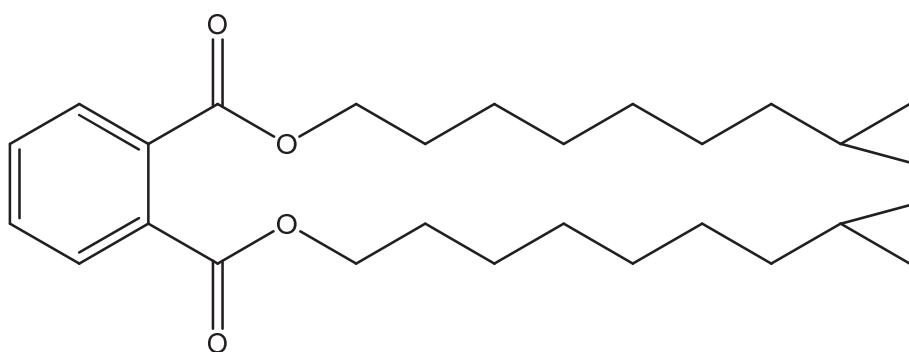


Figure 39: Chemical structure of diisodecyl phthalate.

Table 12: Input values for the HSPs calculations with the group contribution method for DIP.

<i>Group</i>	<i>Quantity</i>	<i>F_d</i> (J ^{1/2} cm ^{3/2} mol ⁻¹)	<i>F_p</i> (J ^{1/2} cm ^{3/2} mol ⁻¹)	<i>U_h</i> (J mol ⁻¹)
-CH ₃	4	419	0	0
>CH-	2	80	0	0
-CH ₂ -	14	270	0	0
-COO- ester	2	667	511	7000
phenyl<	2	1319	133	0

DIP has a molecular weight *M* of 446,67 g/mol and a density ρ of 0,97 g/cm³, resulting in a molar volume *V_m* of 460,5 cm³/mol. Using the equations (4.1) and (3.12) following Hansen Solubility Parameters are obtained:

$$\delta_d = 20,8 \text{ MPa}^{1/2}, \delta_p = 1,6 \text{ MPa}^{1/2}, \delta_h = 3,9 \text{ MPa}^{1/2}, \delta_t = 21,2 \text{ MPa}^{1/2}$$

The δ_h value of DIP is even smaller as this of DEP so that no molecular interactions of DIP with the EMCs are expected. Therefore just the mixture of DIP with BAL was tested. The different distribution of the fractional HSPs between the cured epoxy molding compounds and the phthalates is shown in figure 40.

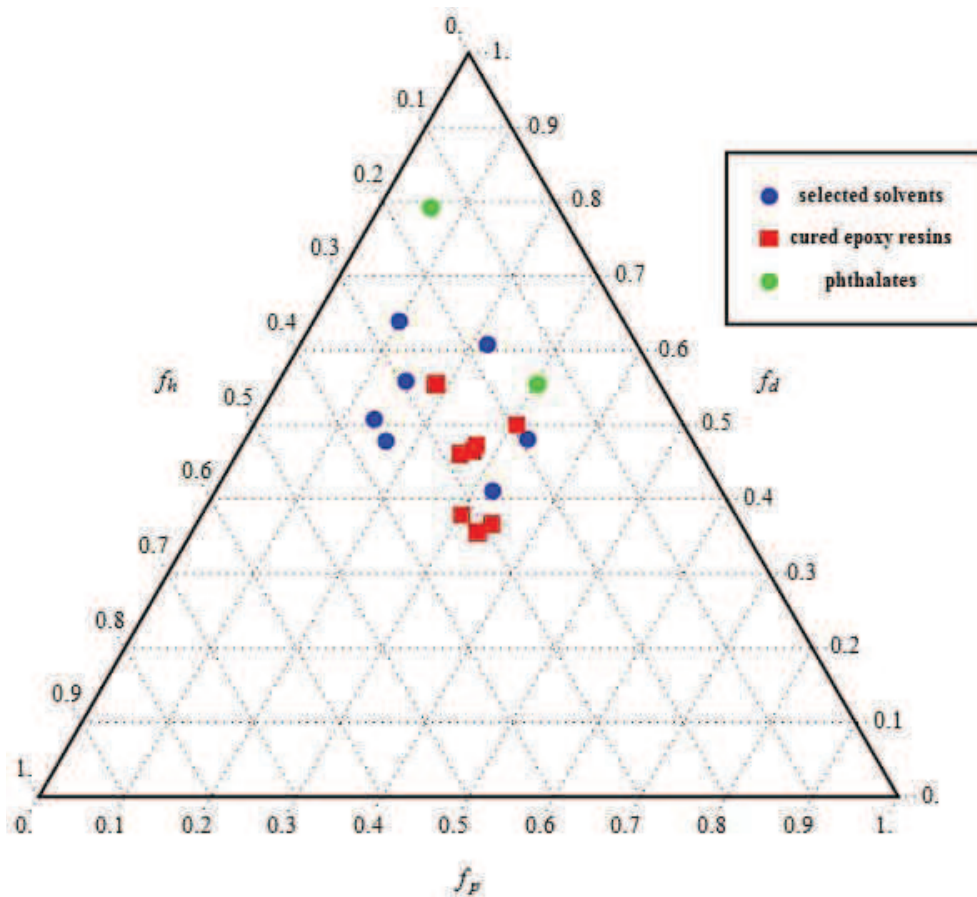


Figure 40: Ternary plot showing the fractional HSPs of the selected solvents, the cured epoxy resins and the used phthalates.

The results of the experimental runs confirmed the statement of the theory of solubility. As phthalates and cured epoxy resins don't have the same distribution of intermolecular forces, they don't interact with each other.

By use of DEP only one package could be decapsulated. The quantity of opened devices could be increased by use of mixtures with BAL or NMP but no positive impact could be

detected by use of phthalates. Although DEP and DIP didn't harm the quality of the die metallization or the polyimide layer they are not suited for the decapsulation of semiconductor devices because no observable modification of the EMCs could be ascertained.

5.6 Multicomponent Runs

Until now it has been shown that among the selected solvents ANI, BAL and NMP were the most promising candidates for solvolysis reactions. DMF also had a positive influence on the EMCs but further experiments with DMF were dropped because packages residues remained on the die surfaces in all experiments. The hydrogen donor IND worked quite well and was kept for further experiments. In the group of supercritical fluids ACE showed a beneficial impact on the preservation of the polyimide layer. The same outcome was achieved with BAT. The addition of BRI had a positive influence on the cleanliness of the die surfaces. Amines were dropped because they attacked the die metallization and phthalates as they didn't show any solvolysis properties. Additionally, two more hydrogen donors, namely tetraline (TET) and dihydroanthracene (DHA), were admitted into the group of solvents to compare their performance with that of IND and because it might be advantageous to use mixtures of hydrogen donors [43].

Combination runs with the most promising candidates were performed to find the best composition for the solvolysis reactions. The mixtures are listed in table 13. All experiments showed very satisfying results. The die metallizations stayed unharmed and all packages could be decapsulated (see figure 41). The only difference was the condition of the polyimide layer. But the addition of different hydrogen donors didn't have any outstanding effects on the EMCs. IND had the best solvolysis behavior.

Experimental Runs and Results

Table 13: Solvent mixtures for the combination runs.

<i>Number</i>	<i>Combination</i>	<i>Amount [mL (g)]</i>
Combi 1	BAL + IND + ACE + BRI	35 + 10 + 5 + 2
Combi 2	BAL + IND + BAT + BRI	40 + 10 + 10 + 2
Combi 3	BAL + TET + BAT + BRI	40 + 10 + 10 + 2
Combi 4	BAL + IND + TET + BRI	40 + 10 + 10 + 2
Combi 5	BAL + IND + DHA	40 + 10 + 2
Combi 6	BAL + BAT + DHA	40 + 10 + 2
Combi 7	BAL + TET + ACE + BRI	35 + 10 + 5 + 2
Combi 8	BAL + IND + TET + ACE	35 + 10 + 10 + 5
Combi 9	BAL + IND + DHA + ACE + BRI	35 + 5 + 5 + 5 + 1
Combi 10	BAL + NMP + IND + BRI	20 + 20 + 10 + 1
Combi 11	ANI + IND + ACE + BRI	35 + 10 + 5 + 1

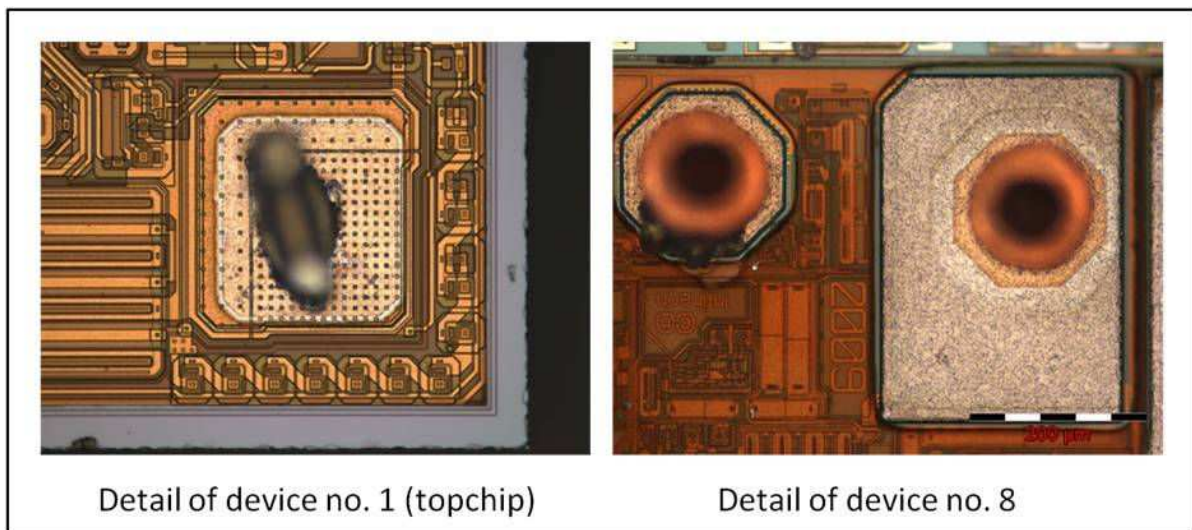


Figure 41: Reflected-light micrographs of device no. 1 (topchip) and device no. 8 after decapsulation using Combi 1. The polyimide layer remained on the die surface.

By use of Combi 1 and 11 the packages were extensively swollen and very easy to decapsulate. Combi 1 was chosen for the optimization of the test parameters because BAL has the advantage over ANI of not being toxic.

5.7 Design of Experiments

For the optimization of the test parameters pressure, temperature and time a design of experiments (DOE) was chosen. A DOE is a systematic approach for the investigation of a system or process, in this case the solvolysis reaction. The predefined input values are statistically varied and a test series in form of a matrix is defined. This method offers a simple way to gain the maximum information about the reaction system. An evaluation of the output values in dependence of one input value alone, as well as input values interacting with one another, is enabled. It can be found out if one input variable alters the effect of another one, so if there are any kinds of dependencies or interactions.

Following input values were chosen:

Initial pressure:	0, 40 and 80 bar.
Reaction temperature:	463, 493 and 523 K.
Reaction time:	7.0, 8.5, 10.0 h.

A full factorial experimental design was chosen to obtain all possible variations of these input values. 23 out of the $3^3 = 27$ runs were performed to fit the model. Combi 1 (see section 5.6) was selected as reaction medium. As it was known that the selected solvent mixture didn't harm the die metallization this output value was substituted by the convenience of the decapsulation procedure.

Following output values were chosen:

Number of opened devices:	0 – 10.
Polyimide layer:	Category 1 – 5 (1 = complete removal, 5 = complete preservation).
Convenience:	1 – 3 (1 = very difficult to decapsulate, 3 = very easy to decapsulate).

Experimental Runs and Results

A predicted response graph was created with the experimental results:

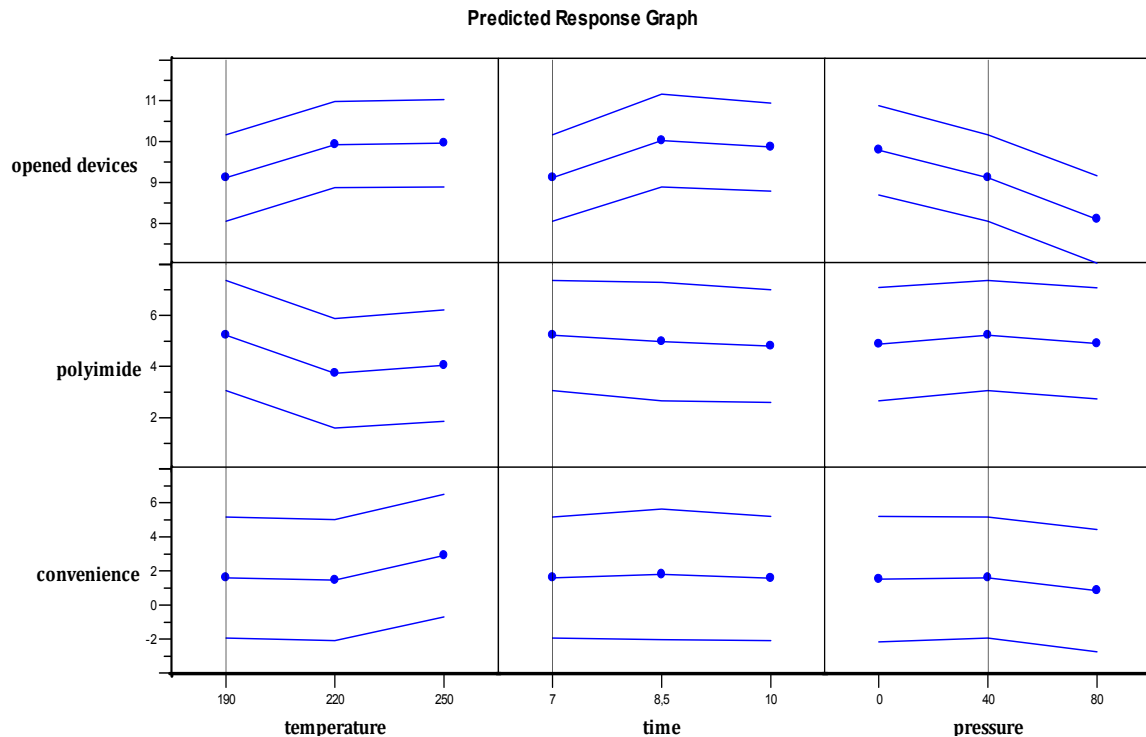


Figure 42: Predicted response graph of the solvolysis reactions using Combi 1.

From figure 42 it can be seen that a temperature of 220 °C or a minimum reaction time of 8,5 hours at 190 °C is necessary to decapsulate all devices. Pressure has a negative influence on the number of opened devices. The condition of the polyimide layer is predominantly dependent on the reaction temperature. The lower the temperature, the more likely is the preservation of the polyimide. The factors time and pressure are of minor relevance for the polyimide layer. The convenience of the opening procedure is enhanced by increasing temperature and decreasing pressure. The time period is too small to affect the convenience.

Effect Pareto charts were created to detect interactions of the input variables (see figures 43 – 45). In the following charts factor F1 stands for temperature, F2 for time and F3 for pressure. Response R1 means number of opened devices, R2 polyimide layer and R3 convenience.

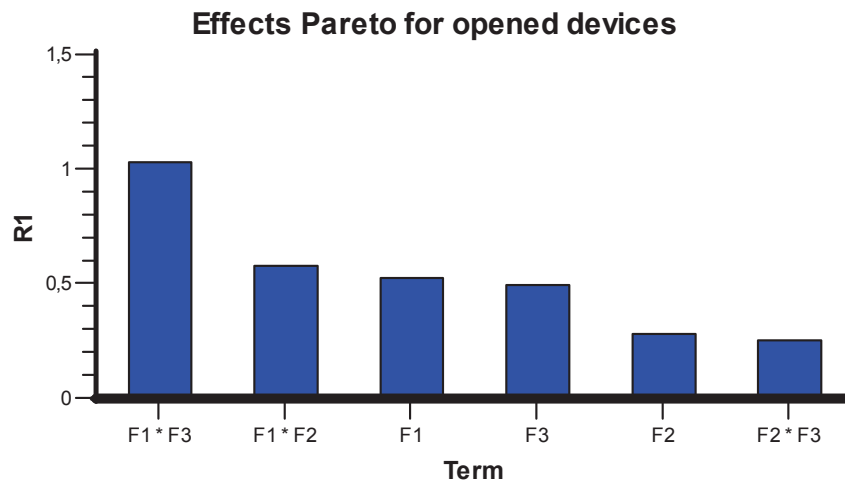


Figure 43: Effects Pareto chart for the number of opened devices.

The number of opened devices is strongly dependent on the interaction of temperature and pressure (see figure 43). The higher the temperature and the lower the pressure, the more swollen is the EMC and the easier is the concomitant decapsulation of the devices.

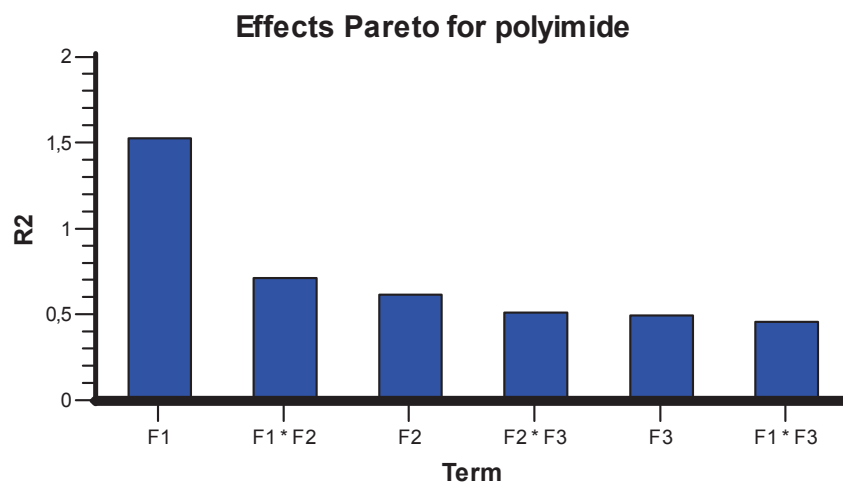


Figure 44: Effects Pareto chart for the preservation of the polyimide layer.

The preservation of the polyimide layer is strongly dependent on temperature (see figure 44). Its dissolution at higher reaction temperatures could be countered by the addition of more ACE or BAT to the reaction mixture. Reaction time and pressure have just a slight influence on the polyimide layer.

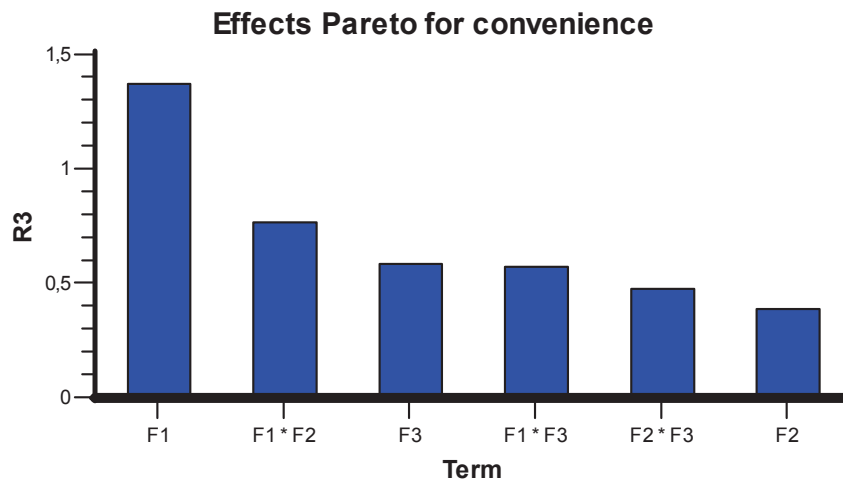


Figure 45: Effects Pareto chart for the convenience of the opening procedure.

The convenience is mostly dependent on the reaction temperature but also improved by longer reaction times and lower pressures.

The DOE has shown that pressure has a negative effect on solvolysis reactions of cured epoxy resins. This is a positive result as the reaction system becomes safer through the omission of initial pressure. In case of a sufficiently long reaction time the temperature can be decreased below 200°C which makes the procedure much gentler for the semiconductor devices.

5.8 Investigation of the Die Metallization

For the investigation of the componential composition of die metallization device no. 4 was decapsulated using Combi 5 (see table 13) and a reference device was decapsulated in a standardized procedure using fuming nitric acid. Both devices were cleaned identically (see section 4.4) and subjected to an EDX analysis (see figure 46).

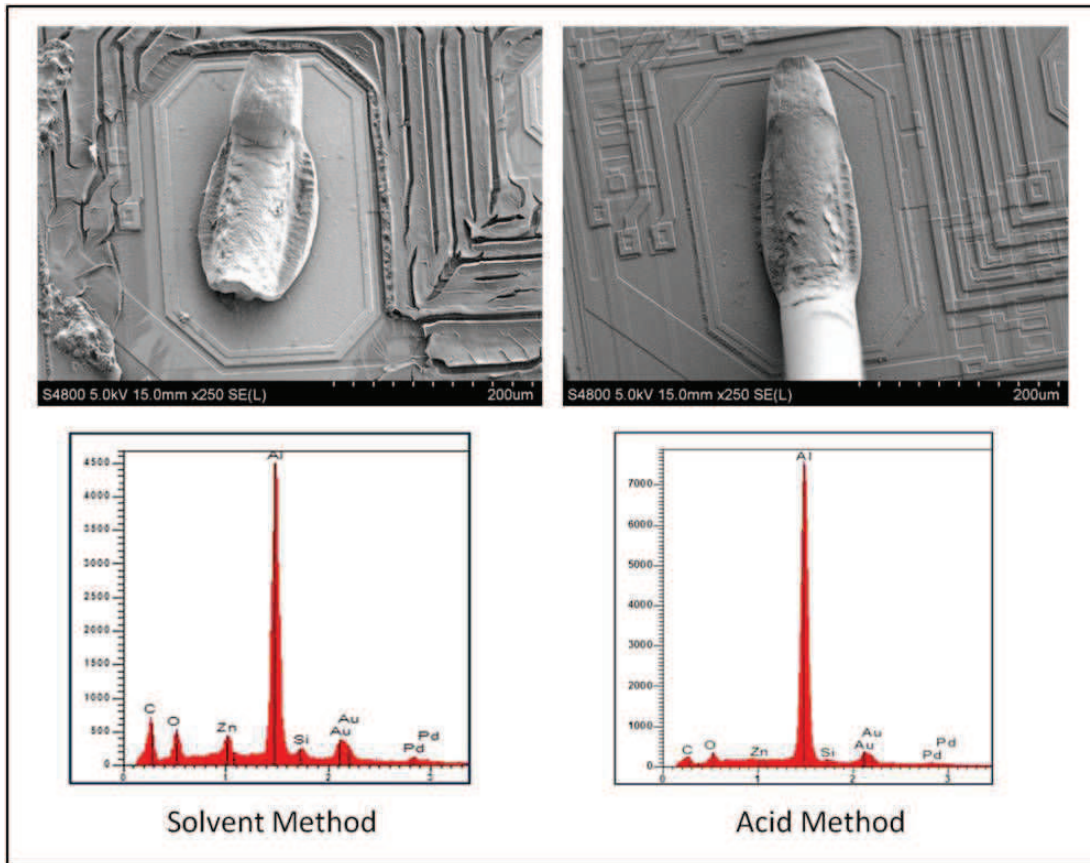


Figure 46: Scanning-electron micrographs and EDX spectra of device no. 4, left after decapsulation using solvents and right after decapsulation using fuming nitric acid.

The scanning-electron micrographs showed that the polyimide layer has not been removed with the solvent method and that the aluminum wire was broken. But the aluminum pads looked the same in both cases. The EDX analysis of the die pads revealed that zinc and silicon traces could be detected by use of the solvent method which were oxidized and washed off by use of acids. Consequently, the solvolysis method is a good approach to prove metal traces, regardless of whether they are purposely deposited to modify adhesion properties or whether they are contaminations from the manufacturing processes.

6 Conclusion

In this work it could be shown that solvent mixtures are a good alternative for the decapsulation of semiconductor devices. Although the epoxy molding compounds are very densely cross-linked and can just be swollen in solvolysis reactions, the packages can be easily decapsulated by use of suited solvent systems. Furthermore the solubility behavior can be predicted with the Hansen Solubility Parameters which facilitates the solvent selection.

Trough the variation of different solvents, e.g. the addition of acetone or butyl acetate, the removal or preservation of the polyimide layer can be directed.

Surfactants have a positive effect on the cleanliness of the die surfaces and the softening of the epoxy molding compound. The effects of further ionic and nonionic surfactants could be investigated.

A drawback of this method is that unveiling of the semiconductor devices is a total decapsulation procedure. The die interconnections are broken and no further electrical analysis is possible.

Pressure has a negative effect on solvolysis reactions. The omittance of pressure makes the reaction system much safer. A horizontal shaker could be installed below the heater to provide a constant mixing of the solvents and to improve the flow dynamics around the test specimens.

Reaction temperature can be decreased to 463 K if the reaction time is long enough, but the opening procedure requires skill from the operator as the convenience is much lower in comparison with 523 K. Different catalysts for transfer hydrogenolysis could be tried out to enhance the reaction rate.

Conclusion

Solvolysis reactions can be applied to provide artifact-free die metallizations which can be investigated by EDX analyses. Metal traces from electrochemical surface refinements as well as impurities from individual process steps can be detected.

All in all the solvolysis of epoxy molding compounds is a good method for special requirements, like the investigation of polyimide layers and die metallizations as well as for copper or aluminum corrosion studies.

Appendix

Information about the used liquids:

liquid	bp [K]	ρ [g/cm]	M [g/mol]	supplier	quality	order number
ACE	329	0,79	58,08	IFAT Villach	n.a.	n.a.
ANI	457	1,02	93,13	Merck	for synthesis	822256
BAL	478	1,05	108,14	Merck	for synthesis	822259
BAT	398	0,88	116,16	Alfa Aesar	99 + %	A19412
DEA	328	0,71	73,14	Sigma-Aldrich	> 99,5 %	31730
DEP	570	1,12	222,24	Alfa Aesar	99%	A17529
DETA	568	0,97	191,28	Merck	for synthesis	817033
DIP	523-540	0,97	446,67	Merck	for synthesis	814732
DMF	426	0,95	73,10	Merck	Lab	103034
IND	493	1,06	119,17	Alfa Aesar	99%	A11000
MeOH	338	0,79	32,04	Merck	for analysis	106009
NMP	476	1,03	99,13	IFAT Villach	n.a.	2121-828-1
TET	473-482	0,97	132,21	Merck	for synthesis	809733
THF	339	0,89	72,11	Merck	for analysis	109731

Information about the used solids:

solid	mp [K]	ρ [g/cm]	M [g/mol]	supplier	quality	order number
BRI	309-315	1,05	1200,00	Merck	for synthesis	801962
DHA	376-380	0,88	180,25	Sigma-Aldrich	97%	126179
SDS	477-480	1,1	288,37	Merck	for synthesis	822050

bp boiling point

ρ density

M molecular weight

mp melting point

Acronyms

ACE	acetone
AlN	aluminum nitride
Al ₂ O ₃	aluminum oxide
ANI	aniline
BAL	benzyl alcohol
BAT	butyl acetate
BN	boron nitride
BPAN	bisphenol A epoxy novolac resin
BPE	biphenyl epoxy resin
BPFN	bisphenol F epoxy novolac resin
BRI	Brij [®] 35
CF ₄	tetrafluoromethane
CMC	critical micelle concentration
DCPD	dicyclopentadienyl resin
DDM	diamino diphenyl methane
DDM _e	tetraethyl derivative of DDM
DDS	diamino diphenyl sulfone
DEA	diethylamine
DEP	diethyl phthalate
DETA	diethyltoluamide
DGEBA	diglycidyl ether of bisphenol A
DHA	dihydroanthracene
DIP	diisodecyl phthalate
DMF	dimethylformamide
DOE	design of experiments
ECN	epoxy cresol novolac resin
EDX	energy dispersive x-ray
EMC	epoxy molding compound
EP	electron pair

Acronyms

Epikote 1001	bisphenol A – epichlorohydrin epoxy resin
EPN	epoxy phenol novolac resin
Epon™	commercially available liquid bisphenol epoxy resin
ER	epoxy resin
FA	failure analysis
HLB	hydrophilic-lipophilic-balance value
HSP	Hansen Solubility Parameter
IMI	imidazole
IND	indoline
LMW	low molecular weight resin
LWA	low water absorption hardener
MAR	multiaromatic resin
MeOH	methanol
MF	multifunctional resin
NMP	N-methyl-2-pyrrolidone
OCN	ortho cresol novolac
P-1700-pSul	bisphenol A – polysulfone resin
PN	phenol novolac hardener
PTFE	polytetrafluoroethylene
RED	relative energy difference
RoHS	restriction of the use of certain hazardous substances in electrical and electronic equipment
RT	room temperature
SDS	sodium dodecyl sulfate
Si ₃ N ₄	silicon nitride
SiO ₂	silicon dioxide
TET	tetraline
THF	tetrahydrofuran
TGAP	triglycidyl derivative of amino phenol
US	ultrasonically
YAG	yttrium aluminum garnet

List of Symbols

α	electric polarizability
${}^{ij}A_{ab}$	acid-base cohesion parameter
c	cohesive energy density
${}^i\chi_{id}$	ideal gas solubility
${}^j\chi_s$	gas solubility in the solvent
δ	Hildebrand Parameter
δ_a	Lewis acid cohesion parameter
δ_b	Lewis base cohesion parameter
δ_d	Hansen Solubility Parameter for dispersion bonds
δ_h	Hansen Solubility Parameter for hydrogen bonds
δ_p	Hansen Solubility Parameter for polar bonds
δ_t	total Hansen Solubility Parameter
${}^{ij}D$	distance of liquid i from the polymer center j
E	electric field strength
ϵ_0	permittivity of vacuum
F_d	group molar contribution of dispersion bonds
f_i	fractional Hansen Solubility Parameter
F_p	group molar contribution of polar bonds
$\Delta_g H$	molar vaporization enthalpy
I	ionization potential
k	Boltzmann constant
K	Kelvin
m	meter
μ	electric dipole moment
μ_i	induced dipole moment
p_c	critical pressure
Φ	volume fraction
ρ_r	reduced density in the supercritical state

List of Symbols

$\rho_{r,l}$	reduced density of the liquid
ppm	parts per million
q	electric charge
r	distance
R	universal gas constant
jR	interaction radius
T	temperature
T_c	critical temperature
U	molar internal energy
$-U$	molar cohesive energy
$-U_d$	disperse cohesive energy
$-U_h$	hydrogen bonding disperse energy
$-{}^iU_i$	energy of dipole-induced dipole interactions
$-U_o$	orientation energy
$-U_p$	polar cohesive energy
$-U_t$	total cohesive energy
${}^i\Delta_g U$	molar vaporization energy
${}_g\Delta_\infty U$	necessary energy for the infinite expansion of saturated vapor
V	volume
iV	molar volume of the liquid
${}^j\bar{V}$	average partial molar volume of the gas in the solvent
V_m	molar volume
W	Watt

Bibliography

- [1] T. H. Tan, N. Mogi, and N. P. Yeoh. Development of environmental friendly (green), thermal enhanced mold compound (TEMC) for advance packages. *International Symposium on Electronic Materials and Packaging*, 160-166, 2000.
- [2] H. Q. Pham, and M. J. Marks. *Epoxy Resins, Ullmann's Encyclopedia of Industrial Chemistry*. Wiley-VCH, 2005.
- [3] <http://www.hitachi-chem.co.jp/english/products/aprm/012.html>, last visited 17th of October 2011.
- [4] L. Nguyen, J. Jackson, C. H. Teo, S. Chillara, C. Asanasavest, T. Burke, R. Walberg, R. Lo, and P. Weiler. Wire sweep control with mold compound formulations. *Electronic components and technology conference, IEEE*, 60-71, 1997.
- [5] M. Narkis, G. Lidor, A. Vaxman, and L. Zuri. New Injection Moldable ESD Compounds Based on Very Low Carbon Black Loadings. *Electrical Overstress/ Electrostatic Discharge Symposium Proceedings, IEEE*, 1-9, 1998.
- [6] <http://www.infineon.com/cms/en/product/technology/green-products/index.html>, last visited 17th of October 2011.
- [7] <http://www.epd-ee.eu/print.php?id=2166>, last visited 17th of October 2011.
- [8] R. Ingkanisorn, and A. Sriyarunya. RoHS-compliant_molding compound evaluation and manufacturability for FBGA packages. *Electronics Packaging Technology Conference, IEEE*, 479-482, 2004.
- [9] A. Aubert, L. Dantas de Morais, and J.-P. Rebrassé. Laser decapsulation of plastic packages for failure analysis: Process control and artefact investigations. *Microelectronics Reliability*, 48(8-9):1144-1148, 2008.
- [10] F. Beck. *Präparationstechniken für die Fehleranalyse an integrierten Halbleiterschaltungen*. John Wiley & Sons, Weinheim, 1988.
- [11] W. Dang, M. Kubouchi, S. Yamamoto, H. Sembokuya, K. Arai, and K. Tsuda. Decomposition Mechanism of Epoxy Resin in Nitric Acid for Recycling. *Environmentally Conscious Design and Inverse Manufacturing, Second International Symposium on Proceedings in EcoDesign 2001:*, 980-985, 2001.
- [12] Z. W. Zhong. Wire bonding using copper wire. *Microelectronics International*, 26 (1): 10-16, 2009.

- [13] W. Robl, M. Melzl, B. Weidgans, R. Hofmann, and M. Stecher. Copper Metallization for Power Devices. *Advanced Semiconductor Manufacturing Conference, IEEE/SEMI*, 259-262, 11th – 12th June 2007.
- [14] S. Murali, N. Srikanth, and C. J. Vath III. An analysis of intermetallics formation of gold and copper ball bonding on thermal aging. *Materials Research Bulletin*, 38 (4):637-646, 2003.
- [15] S. Murali, and N. Srikanth. Acid Decapsulation of Epoxy Molded IC Packages with Copper Wire Bonds. *IEEE Transactions on Electronics Packaging Manufacturing*, 29 (3):179-183, 2006.
- [16] <http://www.nisene.com/jetetch.shtml>, last visited 7th of September 2011.
- [17] www.digit-concept.com, last visited 7th of September 2011.
- [18] D. D. Wilson, and J. R. Beall. Decapsulation of Epoxy Devices using Oxygen Plasma. *15th Annual Reliability Physics Symposium*, 82-84, 1977.
- [19] F. Emmi, F. D. Egitto, and L. J. Matienzo. Etching behavior of an epoxy film in O₂/CF₄ plasmas. *Journal of Vacuum Science and Technology A*, 9 (3):786-789, 1991.
- [20] J. Tang, J. B. J. Schelen, and C. I. M. Beenakker. Optimization of the Microwave Induced Plasma System for Failure Analysis in Integrated Circuit Packaging. *11th International Conference on Electronic Packaging Technology & High Density Packaging*, 1034-1038, 2010.
- [21] M. Pfarr, and A. Hart. The Use of Plasma Chemistry in Failure Analysis. *18th Annual Reliability Physics Symposium*, 110-114, 1980.
- [22] J. Thomas, J. Baer, P. Westby, K. Mattson, F. Haring, G. Strommen, J. Jacobson, S. S. Ahmad, and A. Reinholz. A Unique Application of Decapsulation Combining Laser and Plasma. *Electronic Components and Technology Conference, 2011-2015*, 2009.
- [23] P. Schwindenhammer, P. Poirier, and P. Descamps. Microelectronics Failure Analysis using Laser Ablation of Composite Materials in System in Package. *8th Electronics Packaging Technology Conference*, 752-759, 2006.
- [24] H. B. Kor, A. C. K. Chang, and C. L. Gan. Temperature Control with a Thermoelectric Cooler (TEC) during Laser Decapsulation of Plastic Packages. *17th IEEE International Symposium on the Physical and Failure Analysis of Integrated Circuits*, 1-6, 2010.
- [25] H. Qiu, H. Y. Zheng, X. C. Wang, and G. C. Lim. Laser decapsulation of molding compound from wafer level chip size package for solder reflowing. *Materials Science in Semiconductor Processing*, 8 (4): 502-510, 2005.

- [26] W. J. Byrne. Three Decapsulation Methods for Epoxy Novalac Type Packages. *18th Annual Reliability Physics Symposium*, 107-109, 1980.
- [27] D. Platteter. Basic Integrated Circuit Failure Analysis Techniques. *14th Annual Reliability Physics Symposium*, 248-255, 1976.
- [28] O. Selig, P. Alpern, K. Müller, and R. Tilgner. Thermomechanical Assessment of Molding Compounds. *IEEE Transactions on Components, Hybrids, and Manufacturing Technology*, 15(4): 519-523, 1992.
- [29] R. Klengel, S. Bennemann, J. Schischka, C. Grosse, and M. Petzold. Advanced Failure Analysis Methods and Microstructural Investigations of Wire Bond Contacts for Current Microelectronic System Integration. *European Microelectronics and Packaging Conference*, 1-6, 2009.
- [30] R. Schlangen, R. Leihkauf, U. Kerst, T. Lundquist, P. Egger, and C. Boit. Physical analysis, trimming and editing of nanoscale IC function with backside FIB processing. *Microelectronics Reliability*, 49 (9-11): 1158-1164, 2009.
- [31] M. Jacques. The Chemistry of Failure Analysis. *Annual Proceedings of Reliability Physics Symposium*, 197-208, 1979.
- [32] R. Chen, Q. Zhang, T. Peng, F. Jiao, and S. Liu. Failure Analysis Techniques for High Power Light Emitting Diodes. *12th International Conference on Electronic Packaging Technology and High Density Packaging*, 1-4, 2011.
- [33] A. F. M. Barton. *CRC handbook of solubility parameters and other cohesion parameters*. CRC Press, 1991.
- [34] A. F. M. Barton. *Handbook of polymer-liquid interaction parameters and solubility parameters*. CRC Press, 1990.
- [35] V. Bellenger, E. Morel, and J. Verdu. Solubility parameters of amine-crosslinked aromatic epoxies. *Journal of Applied Polymer Science*, 37:2563-2576, 1989.
- [36] C. M. Tai, T. Gotanda, and K. Tsuda. *Method for recycling of thermoset epoxy resin materials*. European Patent EP 1 085 044 B1, issued 16th of November, 2005.
- [37] H.-H. King, and L. M. Stock. Aspects of the chemistry of donor solvent coal dissolution. The role of phenol in the reaction. *Fuel*, 61(3): 257-264, 1982.
- [38] Y. Kamiya, H. Sato, and T. Yao. Effect of phenolic compounds on liquefaction of coal in the presence of hydrogen-donor solvent. *Fuel*, 57(11): 681-685, 1978.

- [39] G. Curran, R. Struck, and E. Gorin. Mechanism of the hydrogen-transfer process to coal and coal extract. *I & EC process design and development*, 6(2):166-173, 1967.
- [40] D. Braun, W. v. Gentzkow, and A.-P. Rudolf. Hydrogenolytic degradation of thermosets. *Polymer degradation and stability*, 74:25-32, 2001.
- [41] A.-P. Rudolf. *Hydrierende Spaltung von vernetzten Polymeren*. PhD thesis, technische Universität Darmstadt, 2000.
- [42] Y. Sato, Y. Kodera, and T. Kamo. Effects of solvents on the liquid-phase cracking of thermosetting resins. *Energy and Fuels*, 13:364-368, 1999.
- [43] W. v. Gentzkow, D. Braun, and A.-P. Rudolf. *Process for recycling of thermoset materials*. United States Patent US 6 465 702 B1, issued 15th of October, 2002.
- [44] R. Pinero-Hernanz, C. Dodds, J. Hyde, J. Garca-Serna, M. Poliakoff, E. Lester, M. Cocero, S. Kingman, S. Pickering, and K. H. Wong. Chemical recycling of carbon fibre reinforced composites in nearcritical and supercritical water. *Composites: Part A*, 39:454-461, 2008.
- [45] J.-I. Ozaki, S. K. I. Djaja, and A. Oya. Chemical recycling of phenol resin by supercritical methanol. *Industrial and Engineering Chemistry Research*, 39:245-249, 2000.
- [46] H. Tagaya, Y. Shibsaki, C. Kato, J.-I. Kadowaka, and B. Hatano. Decomposition reactions of epoxy resin and polyetheretherketone resin in sub- and supercritical water. *Journal of Material Cycles and Waste Management*, 6(1):1-5, 2004.
- [47] Y. Suzuki, H. Tagaya, T. Asou, J. Kadokawa, and K. Chiba. Decomposition of prepolymers and molding materials of phenolic resin in subcritical and supercritical water under an Ar atmosphere. *Industrial and Engineering Chemistry Research*, 38:1391-1395, 1999.
- [48] M. Goto. Chemical recycling of plastics using sub- and supercritical fluids. *The Journal of Supercritical Fluids*, 47:500-507, 2009.
- [49] Y.-C. Chien, H. P. Wang, K.-S. Lin, and Y. W. Yang. Oxidation of printed circuit boards wastes in supercritical water. *Water Research*, 34(17), 4279-4283, 2000.
- [50] R. D. Smith, C. R. Yonker, J. L. Fulton, and J. M. Tingey. Organized Molecular Assemblies in Supercritical Fluids; Ion Chelates and Reverse Micelles. *The Journal of Supercritical Fluids*, 1:7-14, 1988.
- [51] L. Garcia-Rio, J. C. Mejuto, and M. Perez-Lorenzo. Simultaneous Effect of Microemulsions and Phase-Transfer Agents on Aminolysis Reactions. *The Journal of Physical Chemistry B*, 111:11149-11156, 2007.

- [52] B. Balogh, R. Kovacs, and J. Majsai. Applications and Comparison of Failure Analysis Methods. *29th International Spring Seminar on Electronics Technology*, 14-19, 2006.
- [53] L. Jones. X-Ray Radiographic Techniques in Failure Analysis. *20th Annual Reliability Physics Symposium*, 152-155, 1982.
- [54] A. Teverovsky. Moisture Characteristics of Molding Compounds in PEMs. *NASA technical report, QSS Group, Inc./Goddard Operations*, 2002.
- [55] Anna Regoutz. *Evaluation of Decapsulation Methods for Semiconductor Devices*. Master thesis, Graz University of Technology, 2010.
- [56] http://www.parrinst.com/doc_library/members/4760-catalog.pdf, last visited 5th of October 2011.
- [57] <http://www.parrinst.com/products/non-stirred-pressure-vessels/series-4760-4777/>, last visited 17th of December 2011.
- [58] M. M. Antonijevic, and M. B. Petrovic. Copper Corrosion Inhibitors. A review. *International Journal of Electrochemical Science*, 3:1-28, 2008.
- [59] http://www.sigmaaldrich.com/etc/medialib/docs/Sigma/Instructions/detergent_selection_table.Par.0001.File.tmp/detergent_selection_table.pdf, last visited 22nd of December, 2011.
- [60] V. Hopp. *Grundlagen der chemischen Technologie für Praxis und Berufsbildung*, 4. Auflage, Wiley-VCH, 2001.